LEVEL II

NSWC TR 81-59

AD A104177

A COMPUTER PROGRAM FOR MODELLING WATER ENTRY CAVITY PERFORMANCE AND COMPARISONS OF PREDICTED WITH OBSERVED CAVITIES

BY M. A. METZGER

STRATEGIC SYSTEMS DEPARTMENT

1 FEBRUARY 1981

Approved for public release, distribution unlimited.

NAVAL SURFACE WEAPONS CENTER

Dahlgren, Virginia 22448 • Silver Spring, Maryland 20910

81 9 15 002

UNCLASSIFIED

SECURITY CLASSIFICATION OF THIS PAGE (When Data Entered)

REPORT DOCUMENTATION PAGE

READ INSTRUCTIONS BEFORE COMPLETING FORM

1. REPORT NUMBER: NSWC/TR-81-59	2. GOVT ACCESSION NO.: AD-A104 177
3. RECIPIENT'S CATALOG NUMBER	
4. TITLE (and Subtitle): A COMPUTER PROGRAM FOR MODELLING WATER ENTRY CAVITY PERFORMANCE AND COMPARISONS OF PREDICTED WITH OBSERVED CAVITIES	5. TYPE OF REPORT & PERIOD COVERED: Interim Aug 1980 – Oct 1980
	6. PERFORMING ORG. REPORT NUMBER
7. AUTHOR(s): M. A. Metzger	8. CONTRACT OR GRANT NUMBER(s): 61153N
9. PERFORMING ORGANIZATION NAME AND ADDRESS: Naval Surface Weapons Center, White Oak Laboratory, Silver Spring, MD 20910	10. PROGRAM ELEMENT, PROJECT, TASK AREA & WORK UNIT NUMBERS: 61153N, SR02301, SR0230100, U54AA
11. CONTROLLING OFFICE NAME AND ADDRESS	12. REPORT DATE: 1 February 1981
	13. NUMBER OF PAGES: 64
14. MONITORING AGENCY NAME & ADDRESS (if different from Controlling Office)	15. SECURITY CLASS. (of this report): UNCLASSIFIED
	15a. DECLASSIFICATION/DOWNGRADING SCHEDULE

16. DISTRIBUTION STATEMENT (of this Report)

Approved for public release; distribution unlimited.

17. DISTRIBUTION STATEMENT (of the abstract entered in Block 20, if different from Report)

18. SUPPLEMENTARY NOTES

19. KEY WORDS (Continue on reverse side if necessary and identify by block number)

Computer Program	Vertical	Cavity Flow Model
Computer Simulation	Oblique	Spherical Lamina
Water Entry	Cylinders	Fluid Shell
Water Entry Cavity	Ogives	Surface Pressure
Cavity Study	Axis-Symmetric	Critical Depth

20. ABSTRACT (Continue on reverse side if necessary and identify by block number)

A computer program is presented which is capable of modelling the geometry and performance of the water entry cavity produced by the entry of axially symmetric projectiles. The program is based on an existing theoretical cavity flow model modified to account for atmospheric surface pressure. The computer model is shown to satisfactorily predict cavities produced by vertical and oblique entries (including high-speed entries) from normal air of right circular cylinders and truncated ogives.

DD FORM 1 JAN 73 1473 EDITION OF 1 NOV 65 IS OBSOLETE
S/N 0102-LF-014-6601

UNCLASSIFIED

SECURITY CLASSIFICATION OF THIS PAGE (When Data Entered)

BLANK PAGE

FOREWORD

A computer program is presented which is capable of modelling the geometry and performance of the water entry cavity produced by the entry of axially symmetric projectiles. The program is based on an existing theoretical cavity flow model modified to account for atmospheric surface pressure. The computer model is shown to satisfactorily predict cavities produced by vertical and oblique entries (including high-speed entries) from normal air of right circular cylinders and truncated ogives.

The work reported herein was supported by NAVSEA Code 63R31. The author would like to acknowledge Dr. Thomas Peirce of NAVSEA for his continued interest and support of water-entry research. The author also extends thanks to Dr. John Baldwin and Messrs. Charles W. Smith, Jacob Berezow and Robert Kavetsky for their guidance, advice and support.

F. B. SANCHEZ
By direction

CONTENTS

ILLUSTRATIONS

ILLUSTRATIONS (Contd.)

TABLES

INTRODUCTION

The first part of this report presents the final version of a computer program which is capable of modelling the behavior of the water entry cavity produced at vertical water entry. The program is based on a hydraulic cavity flow model proposed some years ago by G. Birkhoff and R. Isaacs[1] which has been modified to include the effects of an atmospheric surface pressure.

The second part of this report presents a summary of the results of a theoretical and experimental study of the water entry cavity. In this study, observed cavities are compared with cavities predicted by the computer program described in Part 1. Various water entry conditions, covering a wide range of entry velocities, were investigated.

[1]Birkhoff, G. and Isaacs, R., "Transient Cavities in Air-Water Entry," NAVORD 1490 (1951).

BLANK PAGE

PART 1 - CAVITY MODELLING CODE

BACKGROUND

Birkhoff and Isaacs developed two flow models - one which applies to vertical entry and the other to oblique entry. The discussion here will be limited to the vertical entry model on which the program is based. The original model is applicable to the prediction of the open cavity produced by the water entry of axially symmetric missiles from either a vacuum or greatly reduced pressure atmosphere (Abelson[2] found that it also gives good shape predictions of cavities produced by normal air entry up until the time of pullaway).

Birkhoff's vertical entry model is based on the hypothesis that flow "streamlines lie on concentric spherical surfaces centered at the point of impact." Accordingly, the liquid medium can be thought of as being subdivided into infinitesimally thin concentric spherical shells or "laminas" centered at the entry point, as shown in Figure 1. As the missile passes a lamina the fluid within is displaced, or forced, radially outward as shown in Figure 2. The inside edges of the open laminas together form the cavity wall outline. The shells derive their initial kinetic energy from the loss of kinetic energy of the passing missile, resulting from the cavity drag. The cavity drag coefficient of the missile is assumed to remain constant resulting in an exponential velocity decay with depth

$$v_p = v_{p_o} e^{-\alpha r_p} \tag{1}$$

where

v_{p_o} = missile entry velocity

r_p = missile depth

α = retardation coefficient

[2]Abelson, H., "The Behavior of the Cavity Formed by a Projectile Entering the Water Vertically," Ph.D. Thesis, Mechanical Engineering, Univ. of Md., 1969.

Considering a typical lamina located a distance r from the entry point, Figure 3, only the location of the inside edge of the displaced shell, as defined by r and the angle θ_a, is required in order to determine the position of the cavity boundary. By treating the shell as a kind of "fluid pendulum" and utilizing the principle of conservation of mechanical energy, the differential equation relating the angle θ_a to time can be shown to be[1,3]

$$\dot{\theta}_a = \pm \sqrt{\left(\frac{4g}{r}\right) \frac{(\cos \theta_a - \cos \theta_m)}{\sin^2 \theta_a \ln \left[\frac{(2 - \cos \theta_a)(1 + \cos \theta_a)}{\cos \theta_a (1 - \cos \theta_a)}\right]}} \tag{2}$$

where the expression for $\cos \theta_m$ is*

$$\cos \theta_m = \frac{1}{2}\left[2 - \frac{\alpha\, m_p\, V_{p_o}^2\, e^{-2\alpha r}}{\pi\, r^3\, \rho_w\, g}\right] \tag{3}$$

The angle θ_m is the maximum value of the displacement θ_a corresponding to the peak of the lamina's swing. The initial condition can be found by

$$\theta_{a_o} = \theta_a\,(o) = \arctan \frac{R_p}{r} \tag{4}$$

where θ_{a_o}, the initial shell angle, is taken by Birkhoff[1] to be the angle subtended at the point of entry by the zone of separation of the water from the missile surface. This would imply that R_p should be taken as the radius of the missile at the zone of separation. For certain missile configurations it is obvious where the separation occurs and thus what R_p should be (for example, for a right circular cylinder only the nose flat is wetted hence R_p would be taken as half the nose flat diameter). For certain other missile configurations, on the other hand, the location of separation may not be obvious and may be difficult to determine. In such cases it may be necessary to estimate R_p (for example in Abelson's cavity study[3] which involves sphere entries, R_p is taken as the transverse radius of the missile body at its center of gravity, i.e., half the diameter for a sphere).

---

[1]See footnote 1 on page 7.

[3]Abelson, H., "Cavity Shapes at Vertical Water Entry - A Comparison of Calculated and Observed Shapes," NOLTR 67-31 (1967).

*In reference (3) the expression for $\cos \theta_m$ is in error in that the first term in the brackets in Equation (3) appears as a "1" instead of a "2" as it should be. The author, apparently through an oversight, failed to account for the "at rest" potential energy of the shell which, because of the reference datum selected, is not equal to zero. If this at rest term is included in the reference (3) derivation the correct expression for $\cos \theta_m$, with the "2" in the brackets instead of the "1", is obtained.

By differentiating (2) with respect to time the expression for the angular acceleration is obtained:

$$\ddot{\theta}_a = \frac{-2g}{r}\left[\frac{1 + (\cos\theta_a - \cos\theta_m)\,Z}{\sin\theta_a \ln(X)}\right] \tag{5}$$

where:

$$Z = \frac{2 - 4\cos\theta_a}{\cos\theta_a\,(\cos^3\theta_a - 2\cos^2\theta_a - \cos\theta_a + 2)\ln(X)} + \frac{2\cos\theta_a}{\sin^2\theta_a}$$

$$X = \frac{(2 - \cos\theta_a)(1 + \cos\theta_a)}{\cos\theta_a\,(1 - \cos\theta_a)}$$

MODIFICATIONS TO ORIGINAL FLOW MODEL

The foregoing equations, which describe Birkhoff's original model, do not account for pressure either in the cavity or at the water surface since they were assumed to be zero. However, as mentioned earlier, the model as used in the program has been altered to include the effects of surface pressure since this modification is fairly straightforward, providing the surface pressure is regarded as constant. Modifications, on the other hand, to include the effects of pressure in the cavity on cavity behavior are not a simple matter at all.[2] Thus, in the program cavity pressure is assumed to equal zero.

When the effect of surface pressure, P_o, is included it is shown in Appendix 2 that the governing differential equation for the displacement angle θ_a becomes:

$$\dot{\theta}_a = \pm\sqrt{\frac{4\left[rg + (P_o/\rho_w)\right]\left[\cos\theta_a - \cos\theta_m\right]}{r^2 \sin^2\theta_a \ln\left[X\right]}} \tag{6}$$

where, as in the original model, the initial condition is

$$\theta_{a_o} = \arctan\left(\frac{R_p}{r}\right)$$

with corresponding relations for $\ddot{\theta}_a$ and $\cos\theta_m$ as

$$\ddot{\theta}_a = \frac{-2\left[rg + (P_o/\rho_w)\right]}{r^2}\left[\frac{1 + (\cos\theta_a - \cos\theta_m)(Z)}{\sin\theta_a \ln(X)}\right] \tag{7}$$

[2]See footnote 2 on page 9.

and

$$\cos \theta_m = \frac{1}{2}\left[2 - \frac{\alpha\, m_p\, v_{p_o}^2\, e^{-2\alpha r}}{\pi\, r^2\,(r\,\rho_w\, g + P_o)}\right] \tag{8}$$

It can be seen that by setting P_o equal to zero, Equations (6), (7) and (8) reduce to Equations (2), (3) and (5).

Clearly the differential equations for the angle θ_a for both the original and the modified model are non-linear and must be solved for θ_a versus time using numerical integration since analytic solutions for these equations have yet to be found. The program, in fact, solves Equations (6), (7) and (8) using numerical integration.

CAVITY MODELLING

It should be remembered that these lamina equations apply to a single lamina at a distance r from the entry point. Hence, the motion of a lamina at any depth can be found independent of the laminas at the other depths. For this reason the entire cavity may be modelled satisfactorily with the use of a relatively few number of laminas located at selected depths, as shown in Figure 4. The cavity outline at any given time may be obtained easily by plotting the positions of the edges of the laminas, then connecting the appropriate points to get the cavity outline.

Another less accurate, but more convenient method of describing cavity shape, which will represent the cavity for all times, involves plotting the cavity diameter at the selected depths versus time after entry. The result is a set of arc-shaped curves like the ones shown in Figure 8. Obviously, from the figure, deeper laminas start their motion at later times. It can easily be shown that when cavity drag coefficient is constant the time for the missile to reach a lamina at depth r is:

$$t = (e^{\alpha r} - 1)/\alpha v_{p_o}$$

From Figure 5, the diameter of the circular opening in the lamina at a given time is found by the relation

$$D = 2r \sin \theta_a \tag{9}$$

There is an approximation being made here however. Although the diameter computed from Equation (9) is exact, it is actually the diameter of the cavity not at the depth r but at the more shallow depth $r(1 - \cos \theta_a)$ since, from Figure 5, the edge of the lamina rises up as the lamina swings out. For small enough values of the angle θ_a this should present no problem. However, even for fairly large values of θ_a, the approximation should still be reasonable since, in general, the cavity wall is nearly vertical meaning the change in diameter with depth, at a given time, is not that great. A final consequence of using this technique is that at a given depth r, the cavity diameter will never exceed the limiting value 2 r.

The program is designed to make it convenient to implement either of the two modelling techniques mentioned. The output data are in the form of "Spherical Lamina Performance Data" tables where each table corresponds to a lamina at some user specified depth and contains information concerning depth r, θ_a, and Cavity Diameter versus absolute time after entry as well as other auxilliary information such as current model depths and angular velocities and accelerations associated with the shell displacement angle θ_a.

MINIMUM DEPTH RESTRICTIONS. The selection of depths at which to model the cavity cannot be made entirely arbitrarily since the flow model equations break down in the region near the water surface.

For any given entry there is a lamina, located at a critical depth, designated r_{cr_1}, which acquires just enough energy from the passing missile to rise up to where θ_a is equal to 90° (i.e., entry conditions are such that for this particular lamina θ_m is equal to 90°). Needless to say, all laminas at depths less than r_{cr_1} acquire sufficient energy to swing up beyond the point $\theta_a = 90°$. In physical terms such a lamina will continue to swing upward until it flows into itself at the point $\theta_a = 90°$ as depicted in Figure 6. By setting $\cos \theta_m$ in Equation (6) equal to zero (corresponding to $\theta_m = 90°$) and replacing r with r_{cr_1}, the following formula is obtained which can be solved by trial-and-error for the first critical depth r_{cr_1}:

$$0 = \frac{1}{2}\left[2 - \frac{\alpha\, m_p\, V_{p_o}^2\, e^{-2\alpha r_{cr_1}}}{\pi\, r_{cr_1}^2\,(r_{cr_1}\,\rho_w\, g + P_o)}\right]$$

Inspection of Equations (6) through (8) will show that it is safe to model the cavity at depths greater than r_{cr_1}, which assures that the displacement angle θ_a will not exceed 90°. Attempting to model at depths equal to or less than r_{cr_1} will result in a singularity in Equations (6) through (8) when θ_a reaches 90°, although modelling up until this condition occurs may be possible.

A second critical depth, designated r_{cr_2}, occurs nearer to the surface than r_{cr_1}, and is the depth below which Equation (8), for $\cos \theta_m$, breaks down completely. Attempting to model at depths less than r_{cr} will result in a value for $\cos \theta_m$ which is less than -1. Even so, as in the case of the first critical depth, Equations (6) through (8) still "work" until θ_a reaches 90° (where the singularity occurs) although it is not known at this time if the results produced will be meaningful.

Figure 7 summarizes the minimum depth restrictions. Since these restrictions apply to depths in a small region near the water surface they should not, in general, interfere with the modelling of the overall cavity.

PROGRAM DESCRIPTION

The computer program is written in standard FORTRAN and a listing of it appears in Appendix 1. The first part of the listing is essentially a "user's manual." To demonstrate the use of the program a sample problem has been carried out in the next article. A brief description of the program is given here.

Basically the program solves the lamina motion Equation (6), (7) and (8) for θ_a with time for the lamina at each user specified depth using the three term taylor series:

$$\theta_{a(i+1)} = \theta_{a(i)} + \dot{\theta}_{a(i)} \Delta t + \frac{1}{2} \ddot{\theta}_{a(i)} (\Delta t)^2$$

Currently, the maximum allowable number of depths which may be specified is 10, however this number may be increased simply by increasing the Fortran DIMENSION parameters for the variables DEPTH, DELTA and NSTORE as required. The end result of the computations for a lamina at a particular depth is the single "Spherical Lamina Performance Data" table described in the previous section. There are no "Max Time" or "Max Iterations" parameters to bother with since, when the motion of a particular lamina is completed, the sign of the angle θ_a goes negative, and the computations for that lamina are terminated automatically. A sample of the data tables appears in Appendix 1 following the program listing. These tables are the results for the sample problem described next.

SAMPLE PROBLEM

The program was used to model the cavity produced by the water entry of a steel right circular cylinder, 1.50" diameter by 2.15" long, from normal air, at an entry speed of 250 feet/second. The cavity was modelled with laminas at depths of 10, 20 and 30 calibers. Several test runs were carried out, using progressively smaller values for the time step, until convergence to the solutions for all three laminas was obtained. The results of the final run can be found in Appendix 1 following the program listing. The first page of the output is a Reference Information table listing data describing the entry conditions. Following the Reference Information are the three "Spherical Lamina Performance Data" tables for the laminas at each of the selected depths. The data in these tables were used to generate the curves, in Figure 8, of cavity diameter history at each of the three depths.

PART 2 - CAVITY STUDY

BACKGROUND

G. Birkhoff[1] compared cavities predicted by his original model for vertical entry with experimental data concerning a one inch diameter steel sphere entering water vertically from a reduced pressure atmosphere at a velocity of 73 feet/second with a surface pressure of 1/27 atmosphere.

Abelson[3] compared the cavities predicted by Birkhoff's model to those generated by the vertical entry of spheres into water from reduced pressure atmospheres. The spheres had diameters of either 0.5 or 1.0 inches and entry speeds of between 62 and 69 feet/second.

Initially, Birkhoff's original model was applied only to open cavities produced by entry from a vacuum or reduced pressure atmosphere. Then Abelson[2] compared the model to the cavity produced by a normal air entry and found that theoretical and observed cavity shapes agreed well up until the time of pullaway. Abelson then modified the model to include the effects of both constant surface pressure and a measured cavity pressure. He then compared the cavities predicted by the altered model to the observed normal air entry cavities and found that the modified model predicted cavity shapes which were, in fact, considerably smaller in size than both the observed cavities or those predicted by the original model. The fact that Birkhoff's original model, unaltered for system pressure, satisfactorily predicts cavities produced by both normal and reduced pressure entries suggested to Abelson that cavity shape might be practically independent of surface or cavity pressure, at least up to the time of pullaway. In an attempt to confirm this hypothesis, Abelson compared the cavities produced by sphere entries from both normal and reduced pressure atmospheres and found that "the cavities were identical until surface closure and then began to deviate increasingly until pullaway, with the cavities of the reduced pressure entries slightly larger." As a result of his observations, Abelson concluded that the cavity shape is in fact practically independent of surface or cavity pressure up to the time of pullaway and hence, that Birkhoff's original model is the one to use to satisfactorily predict cavity shape and that "any modification of the model to include system pressure invalidates it."

---

[1]See footnote 1 on page 7.

[2]See footnote 2 on page 9.

[3]See footnote 3 on page 10.

EXPERIMENTAL/THEORETICAL STUDY

Comparisons of Birkhoff's vertical entry model to experiment are limited mostly to shots involving spheres entering at relatively low velocities (below 73 feet/second). An exception is Abelson's comparison of the model to the case of a water entry involving a 3 inch diameter cylindrical missile having a 140 degree conical nose, entering at 200 feet/second from normal air.[2] In view of these limitations it was felt that it would be useful to compare both the original model and the version modified for surface pressure (in spite of Abelson's conclusion that inclusion of system pressure invalidates the model) to entries involving higher velocities and model configurations other than spheres.

Specifically, theoretical cavities predicted by the models were compared to observed cavities from a number of shots involving normal air pressure entries of right circular cylinders of various diameters and aspect ratios and also to shots involving cylindrical missiles of various sizes having truncated ogive nose configurations.

One source of experimental data was photographic records from vertical water entry tests conducted in the NSWC Pilot Tank Facility in 1967 under the supervision of Dr. A. May.[4] The shots chosen for this study involved right circular cylinders and stepped right cylinders.* Model and test condition data for the shots chosen from May's test for this study are given in Table 1. Nose flat diameters ranged from 0.9 to 1.5 inches and entry velocities ranged from 175 to 415 feet/second.

High-speed motion pictures from another water entry test program, conducted in the NSWC Undersea Weapons Tank around 1959, provided a second source of experimental data.[5] This test series involved high speed oblique entries of truncated ogives and right circular cylinders. Although these shots involved oblique entries it was felt that, for the depths of interest in this study (below 50 calibers**), the entry angles of 45, 47 and 70 degrees (from horizontal) were steep enough that changes in the cavity geometry, as compared to a vertical entry, would not be appreciable. For the shots chosen from the series for this study the entry model nose flat diameters ranged from 0.707 to 1.570 inches and entry velocities ranged from 426 to 1175 feet/second. Model and test condition data are given in Table 2.

---

[2] See footnote 2 on page 9.

[4] May, A., "The Cavity After Vertical Water Entry," NOLTR 68-114 (1968).

[5] May, A. and Hoover, W. R., "A Study of the Water-Entry Cavity," NOLTR 63-264 (1963).

*For the two shots involving the stepped cylinders, the stepped shoulder remained within the cavity and was not observed to interfare in any way with cavity production.

**Based on nose flat diameters.

TABLE 1

MODEL AND TEST CONDITION DATA: PILOT TANK SERIES

SHOT #	MODEL CONFIG.	NOSE FLAT DIA. (in)	MODEL LENGTH (in)	MODEL WT. (lbs)	MAT'L.
1419	RIGHT CIRC. CYL.	1.000	8.25	1.834	STEEL
1711	RIGHT CIRC. CYL.	1.500	2.00	2.143	UNKNOWN
1438	RIGHT CIRC. CYL.	1.500	4.39	2.195	STEEL
1434	RIGHT CIRC. CYL.	1.500	2.15	1.075	STEEL
1474	SINGLE STEPPED CYL.*	0.900	10.10**	1.818	STEEL
1476	SINGLE STEPPED CYL.*	0.900	10.10**	1.818	STEEL

SHOT #	ENTRY VELOC. (ft/sec)	DRAG AREA (sq in)	CAVITY DRAG COEFF.	ENTRY ANGLE
1419	175.0	.785	.807	VERTICAL
1711	200.3	1.767	.807	VERTICAL
1438	245.0	1.767	.807	VERTICAL
1434	250.0	1.767	.807	VERTICAL
1474	320.0	0.636	.807	VERTICAL
1476	415.0	0.636	.807	VERTICAL

*Stepped cylinder dimensions: 0.90" dia x 0.975" long nose cylinder;
1.50" dia. x 3.308" long body cylinder.

**Length for an equivalent steel unstepped cylinder (i.e., one having the same weight and nose flat diameter of the stepped cylinder).

TABLE 2

MODEL AND TEST CONDITION DATA: UNDERSEA WEAPONS TANK SERIES

SHOT #	MODEL CONFIG.	NOSE FLAT DIA.* (in)	MODEL LENGTH (in)	MOD WT. (lbs)	MAT'L.
184	TRUNCATED OGIVE	0.707"	NOT AVAILABLE	1.599	NOT AVAILABLE
192	TRUNCATED OGIVE	0.864	NOT AVAILABLE	1.600	NOT AVAILABLE
205	TRUNCATED OGIVE	.774	NOT AVAILABLE	1.669	NOT AVAILABLE
193	TRUNCATED OGIVE	.864	NOT AVAILABLE	1.600	NOT AVAILABLE
63	TRUNCATED OGIVE	.785	NOT AVAILABLE	1.652	NOT AVAILABLE
172	RIGHT CIRC. CYL.	1.570	NOT AVAILABLE	1.537	NOT AVAILABLE

SHOT #	ENTRY VELOC. (ft/sec)	DRAG AREA (sq in)	CAVITY DRAG COEFF.	ENTRY ANGLE** (deg)
184	426.0	.393	.800	47.0
192	548.0	.586	.800	47.0
205	599.0	.471	.800	47.0
193	832.0	.586	.800	47.0
63	946.0	.484	.800	70.0
172	1175.0	1.936	.800	45.0

*For these models full body diameters were equal to 1.57 inches.

**Angle between theoretical gun line and water surface.

SUMMARY OF RESULTS

All together, twelve water entries were modelled with results presented in the form of cavity diameter histories shown in Figures 9 through 23. The curves in Figures 9 through 20 compare observed cavities with cavities predicted by the altered theoretical model which includes effects of surface pressure. The remaining curves in Figures 21 through 23 compare observed cavities with cavities predicted by Birkhoff's original model. Each graph contains cavity diameter time histories for both predicted and observed cavities at selected depths. The data in nearly all the plots extend well beyond the time of pullaway (the only exception is shot #172 where a deep closure occurred and no pullaway was observed). Time data were obtained from timing marks present on the film.

For the curves in Figures 9 through 23, corresponding to the study with surface pressure, the following observations were made:

1. In general the model altered for surface pressure appears to underestimate the cavity diameter, hence cavity size. This observation should be expected to some degree since cavity presure is assumed to be zero. The exceptions are shots #63 and #1476. In both these cases curves for observed and predicted cavities agree closely for all depths for roughly the first half of the curves, corresponding to cavity growth, then for the last half, corresponding to cavity collapse, the model overestimates the diameters.

2. Model correctly predicts a deep closure type of collapse (collapse from the bottom up) for shot #172 and base closure type collapse (collapse from top of the cavity downward) for the remaining shots.

3. Theoretical "lag times" (times needed for missile to reach selected depths) which have nothing to do with the model but result from the assumption of constant cavity drag coefficient, agree well with observed lag times.

Following the cavity diameter histories is a set of curves in Figure 24 showing the results of a parametric study of the surface pressure P_0 to determine the sensitivity of cavity size, at a representative depth of 20 calibers, to variations in surface pressure.

The cavity diameter histories in Figure 25 are for a theoretical cavity predicted by Birkhoff's original model. It is included to show how the typical theoretical cavity behaves since, for the study involving the original model in Figures 21 through 23 only a small portion of the theoretical curves could be shown on the graphs because of their extremely long periods, as compared to the experimental curves. The diameter histories in Figure 25 (essentially an extension of the theoretical curves in Figure 15 for shot #1474) indicate that a deep closure occurs at a depth of 140 calibers.

RECOMMENDATIONS

The following recommendations suggest areas to consider for future work and items which may be of concern in a more involved study:

1. Some years ago, according to H. K. Steves, there were shots done in the NSWC Hydro-Ballistics Tank Facility involving high speed vertical entries which are recorded on film. It may be useful to see how well cavities produced by the model compare with these cavities since the high speed shots considered in this study involved oblique entries whereas the flow model is intended to be applied to vertical entries.

2. Reread the photographic records for the vertical entries in Figures 21 through 23 to determine approximately when the time of pullaway occurs and indicate these times on the graphs. Then compare the results in these curves with Abelson's suggestion that cavity shape can be satisfactorily predicted up until pullaway for normal air entries using Birkhoff's original model.

3. Modifications should be made to the current version of the cavity modelling code to enable it to handle the problems associated with modelling the cavity in the critical minimum depth region. Currently no such capability exists in the code, consequently programming difficulties related to the numerical complications described earlier will arise if an attempt is made to model in this region. At the very least, changes could be made to the code so that it will simply ignore specified depths which fall within the critical region and, in addition, issue a message warning the user of the condition. More sophisticated modifications could allow some limited modelling within this critical region.

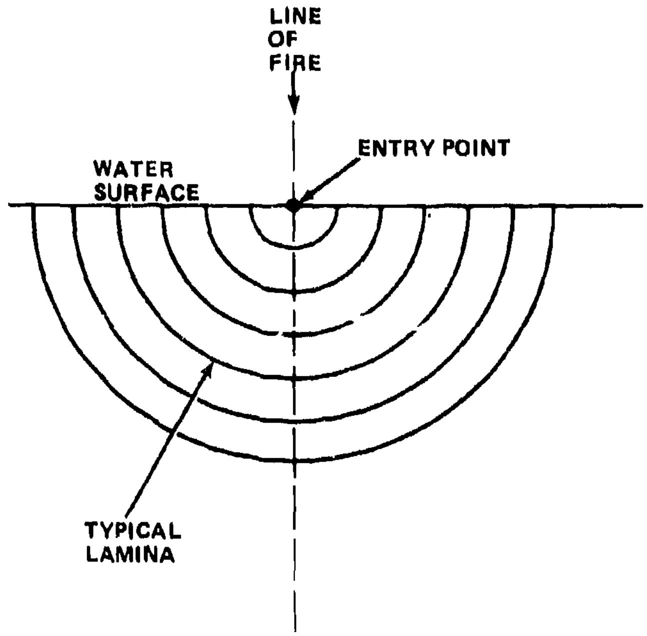

FIGURE 1 LIQUID MEDIUM SHOWN SUB-DIVIDED INTO CONCENTRIC SPHERICAL SHELL OR "LAMINA" REGIONS

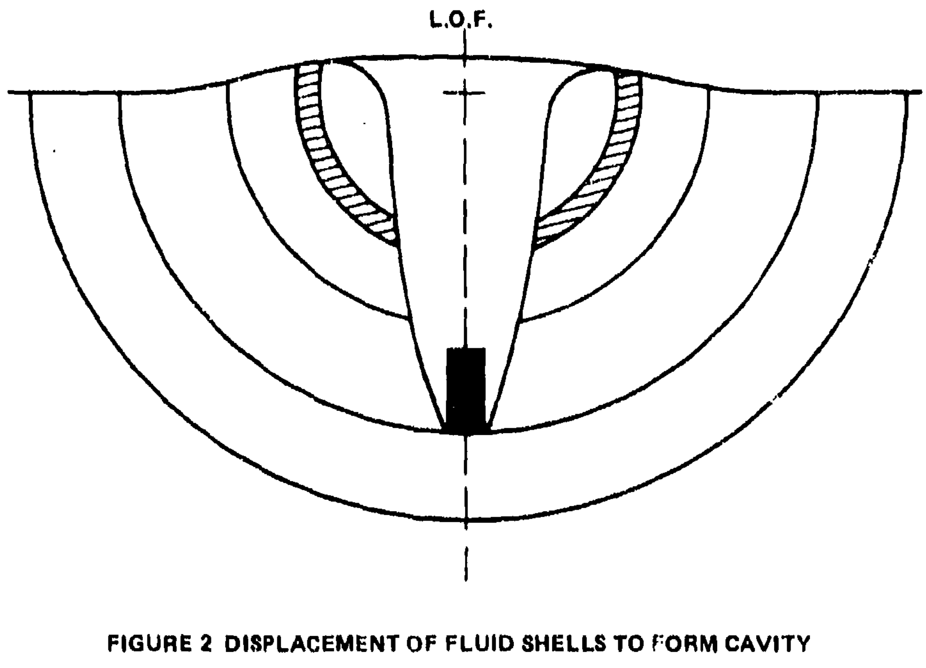

FIGURE 2 DISPLACEMENT OF FLUID SHELLS TO FORM CAVITY

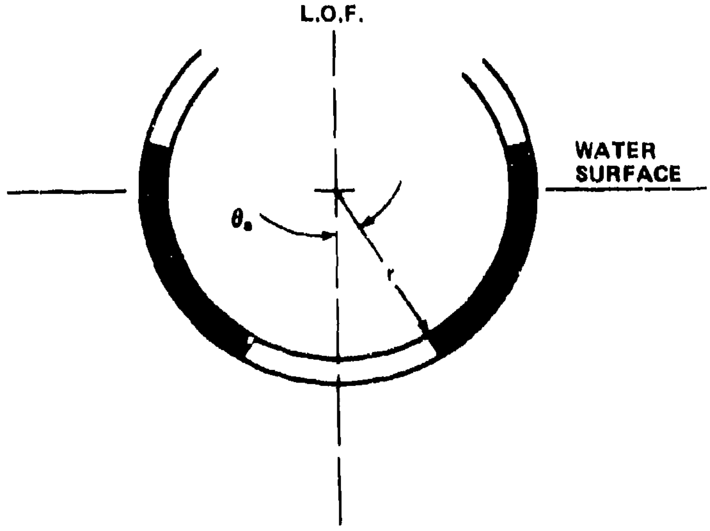

FIGURE 3 FLUID LAMINA GEOMETRY

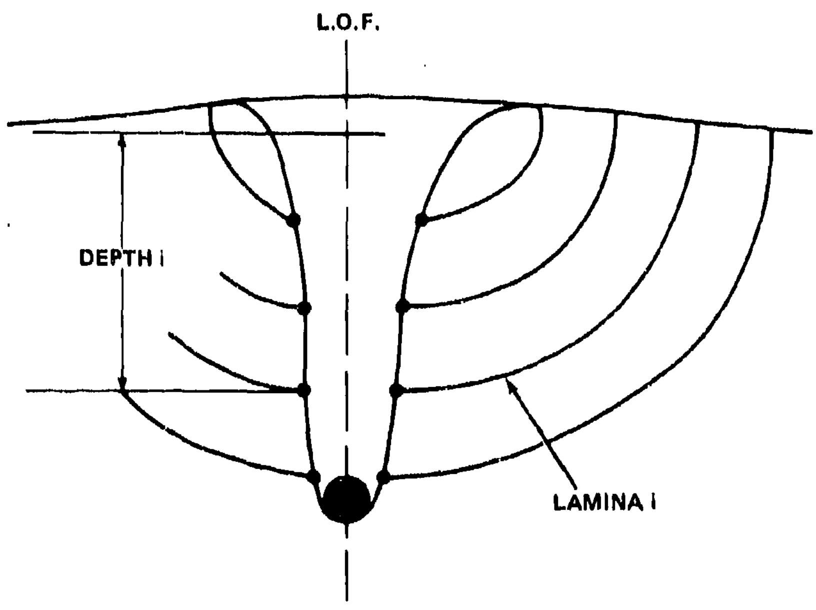

FIGURE 4 MODELLING THE CAVITY WITH THE USE OF LAMINAS AT SELECTED DEPTHS

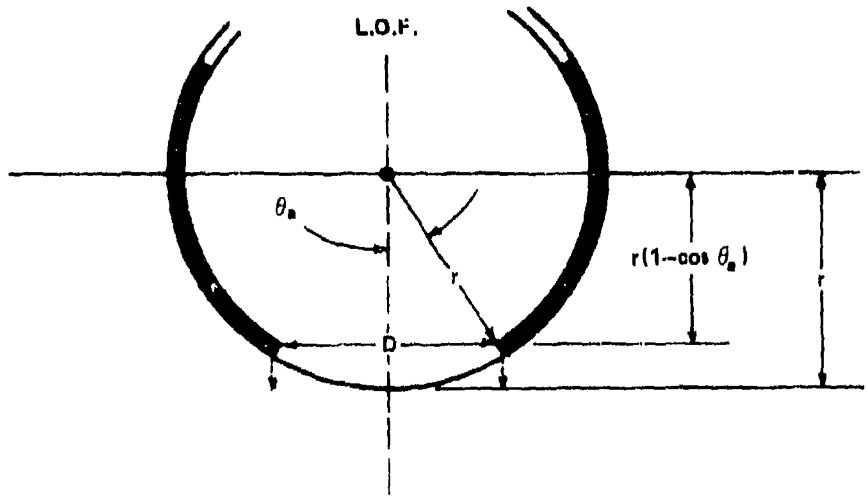

FIGURE 5 CAVITY DIAMETER APPROXIMATION. DIAMETER AT DEPTH r APPROXIMATED BY PROJECTING D DOWN TO DEPTH r

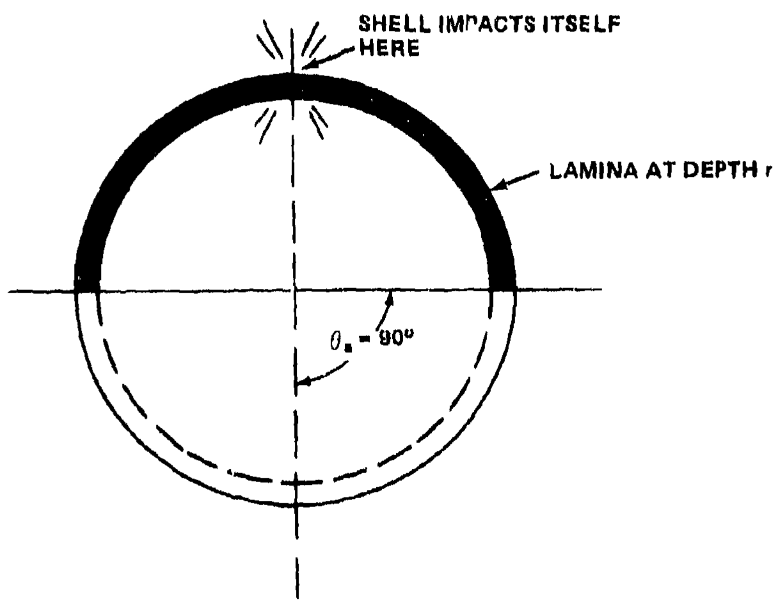

FIGURE 6 FLUID SHELL IMPACTING ITSELF

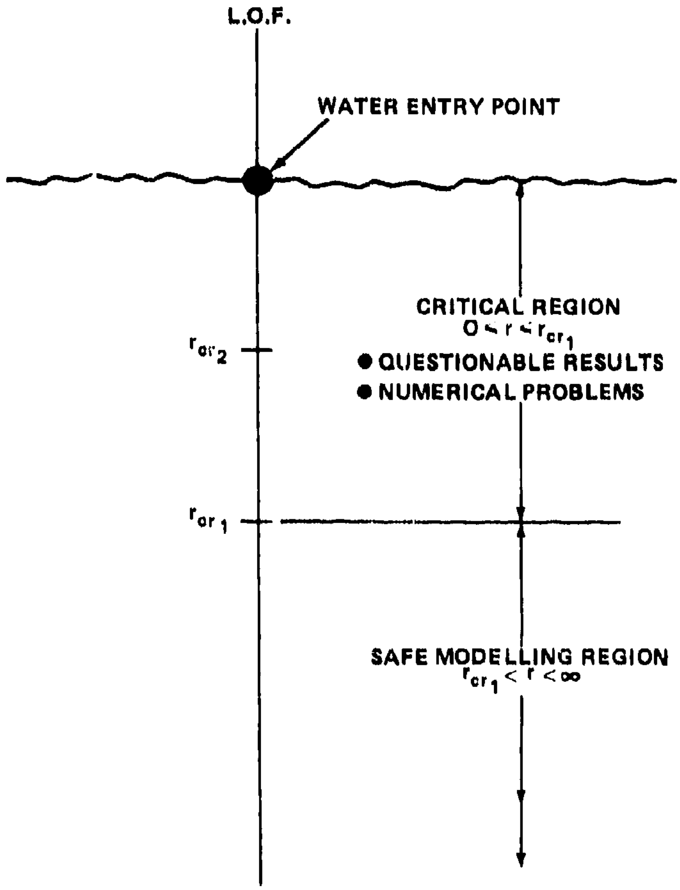

FIGURE 7 SUMMARY OF CRITICAL MINIMUM DEPTH RESTRICTIONS

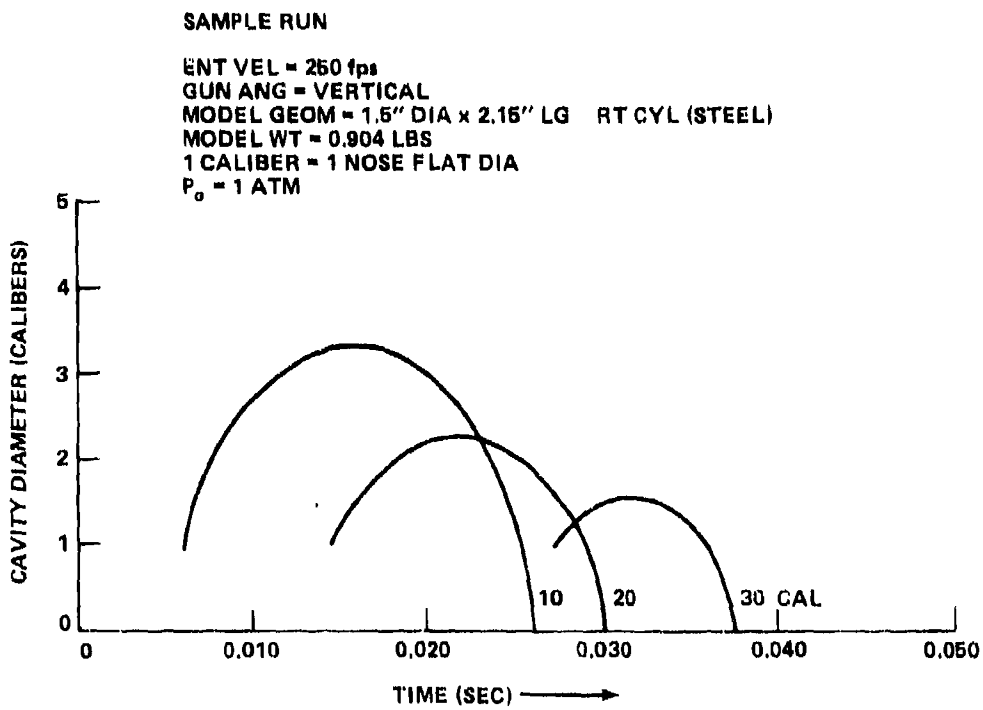

FIGURE 8 CAVITY DIAMETER AT VARIOUS DEPTHS VS TIME

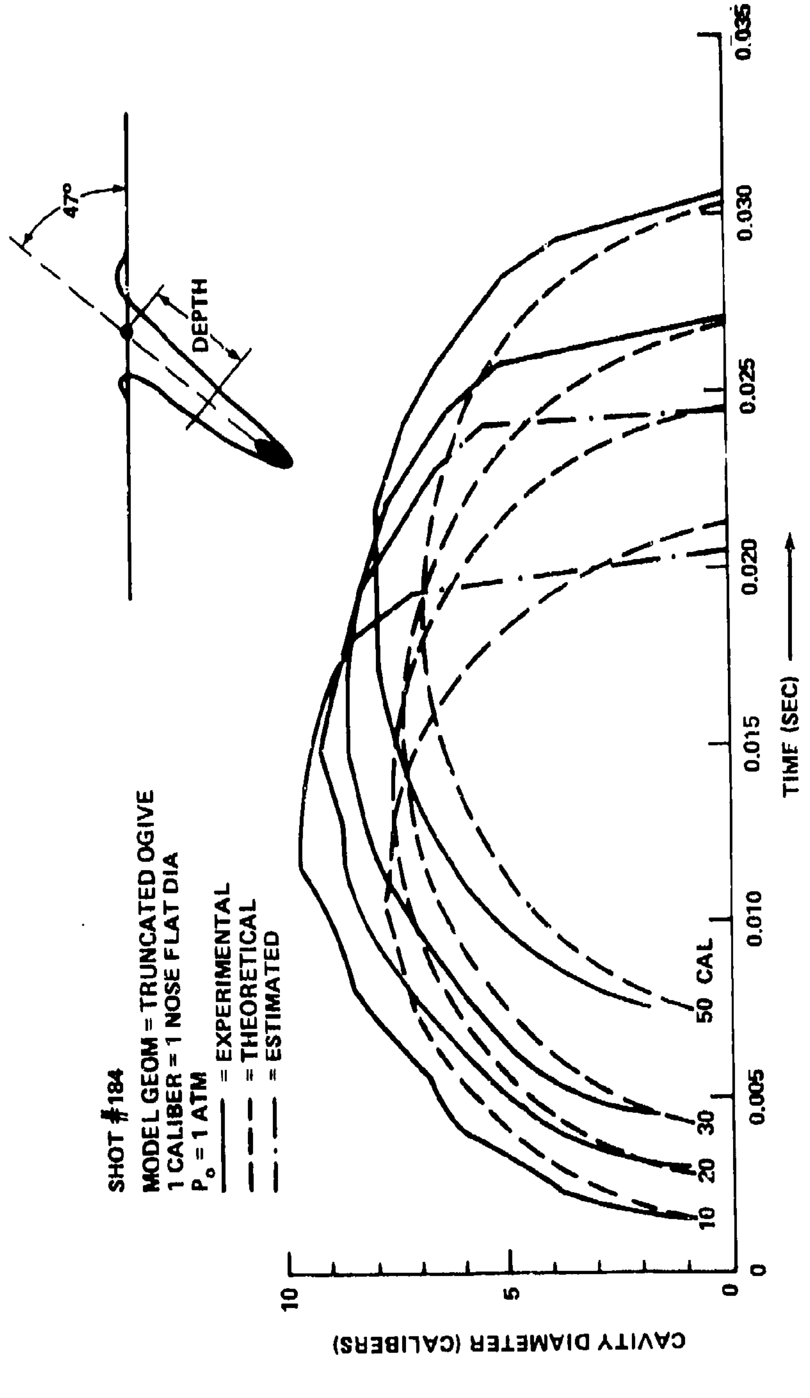

FIGURE 9 CAVITY DIAMETER AT VARIOUS DEPTHS VS TIME

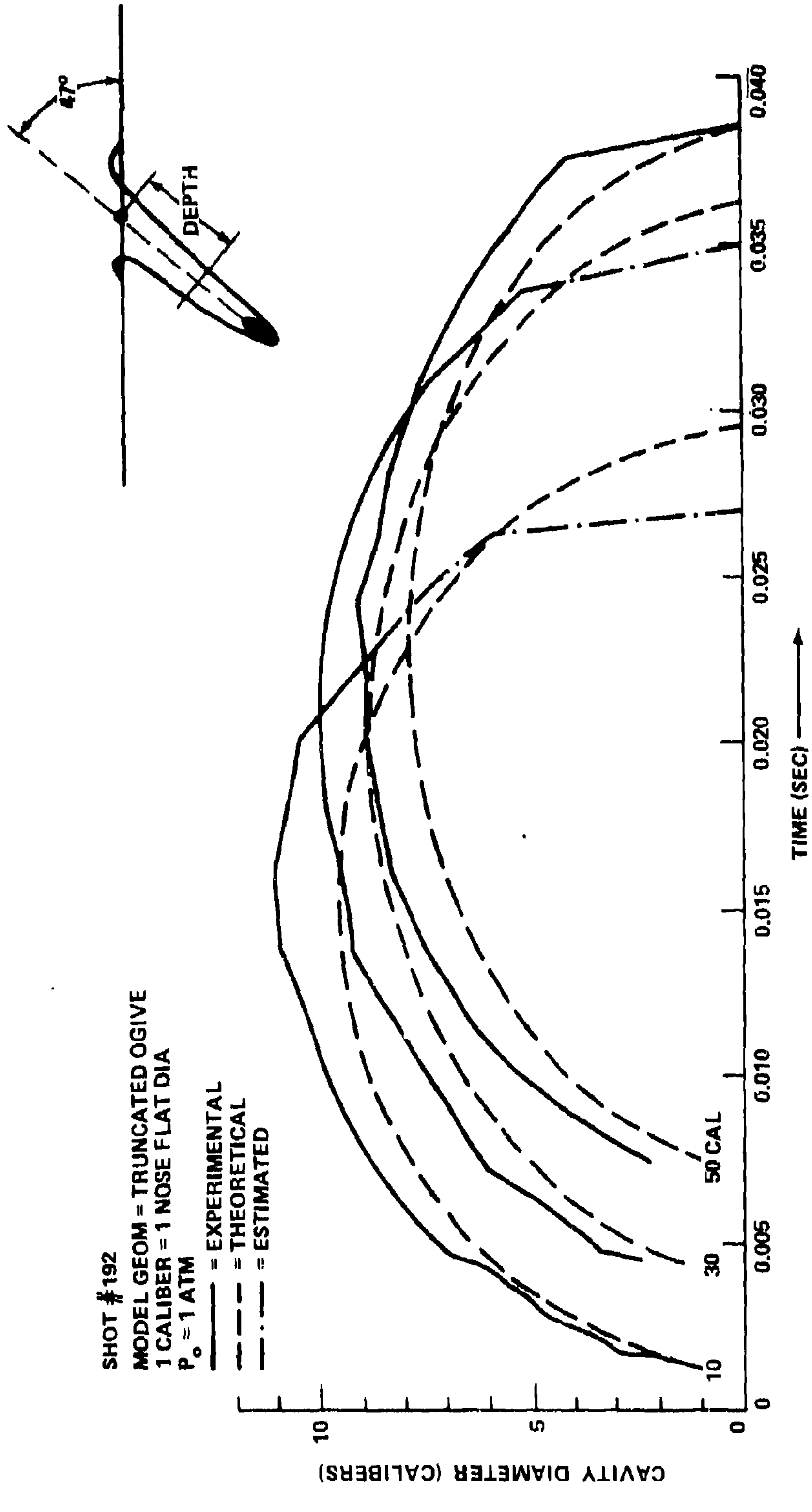

FIGURE 10 CAVITY DIAMETER AT VARIOUS DEPTHS VS TIME

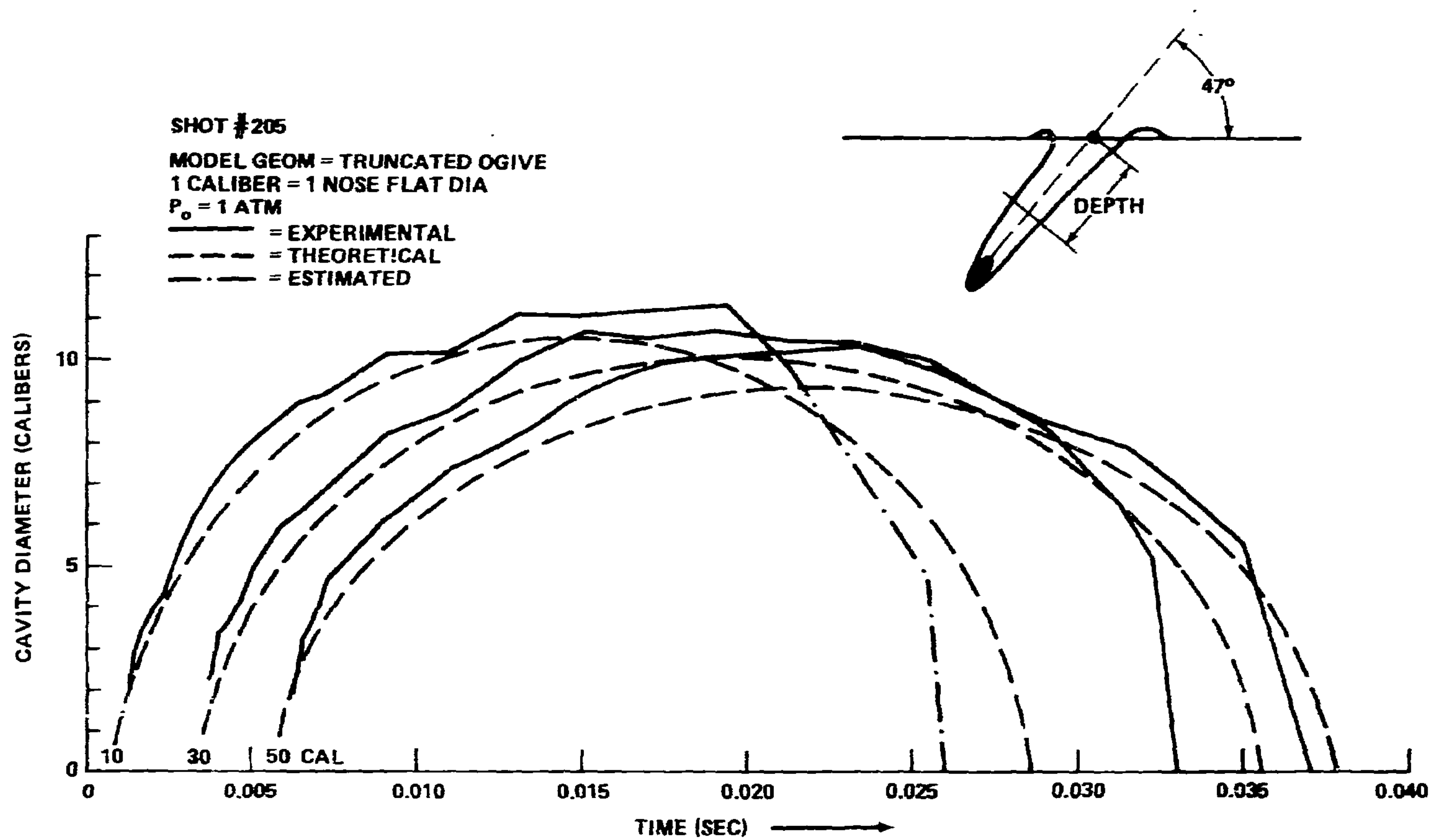

FIGURE 11 CAVITY DIAMETER AT VARIOUS DEPTHS VS TIME

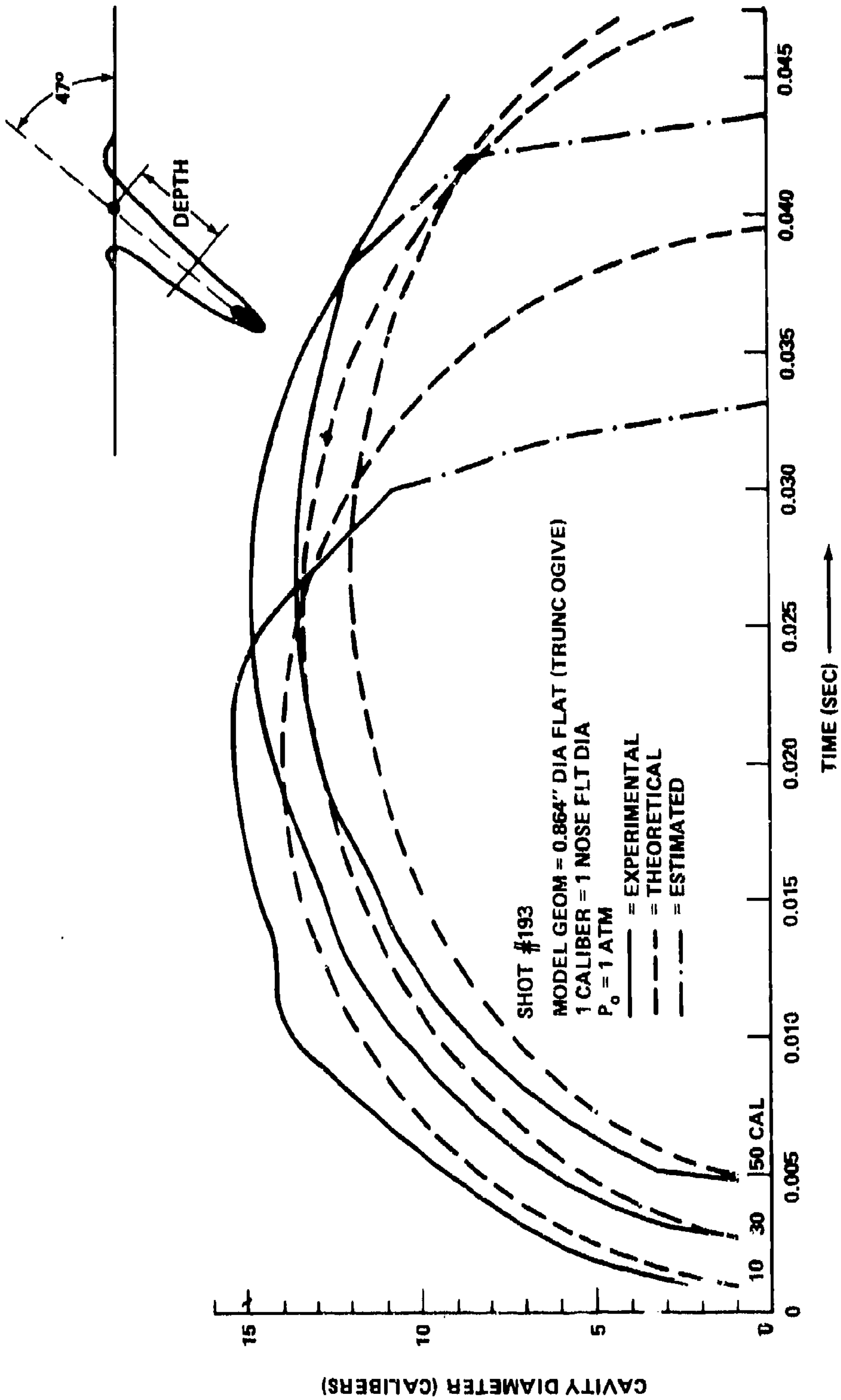

FIGURE 12 CAVITY DIAMETER AT VARIOUS DEPTHS VS TIME

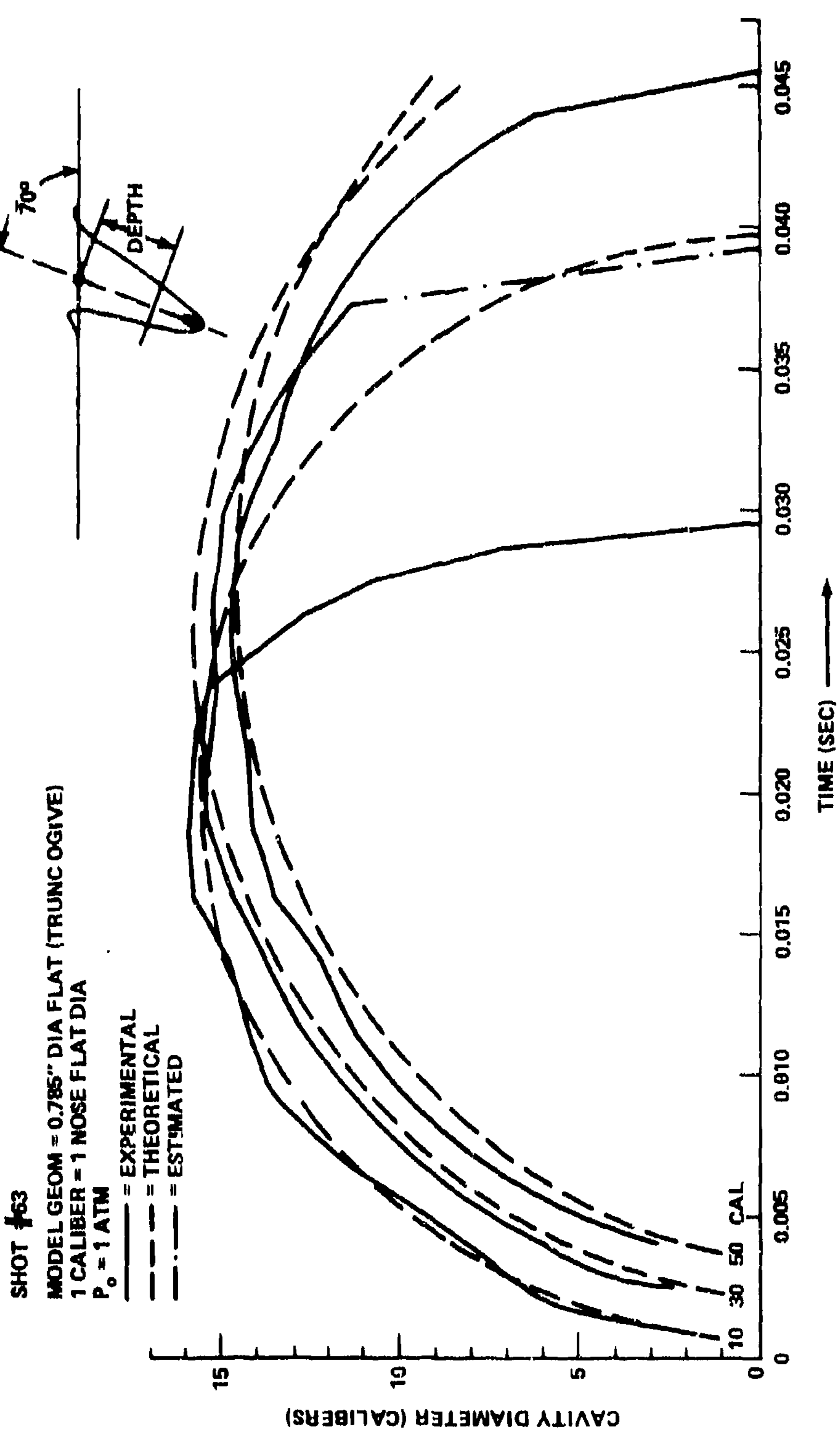

FIGURE 13 CAVITY DIAMETER AT VARIOUS DEPTHS VS TIME

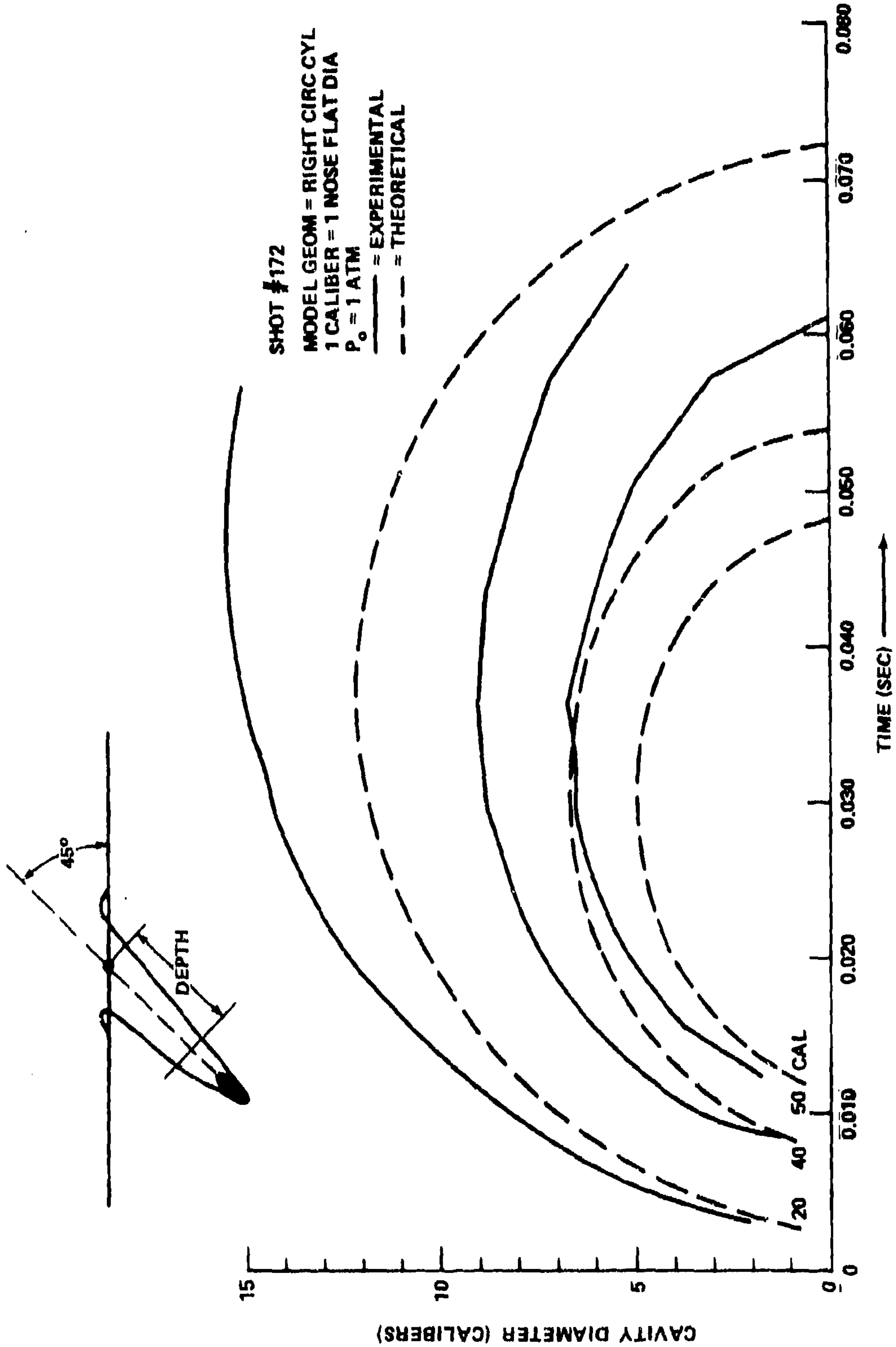

FIGURE 14 CAVITY DIAMETER AT VARIOUS DEPTHS VS TIME

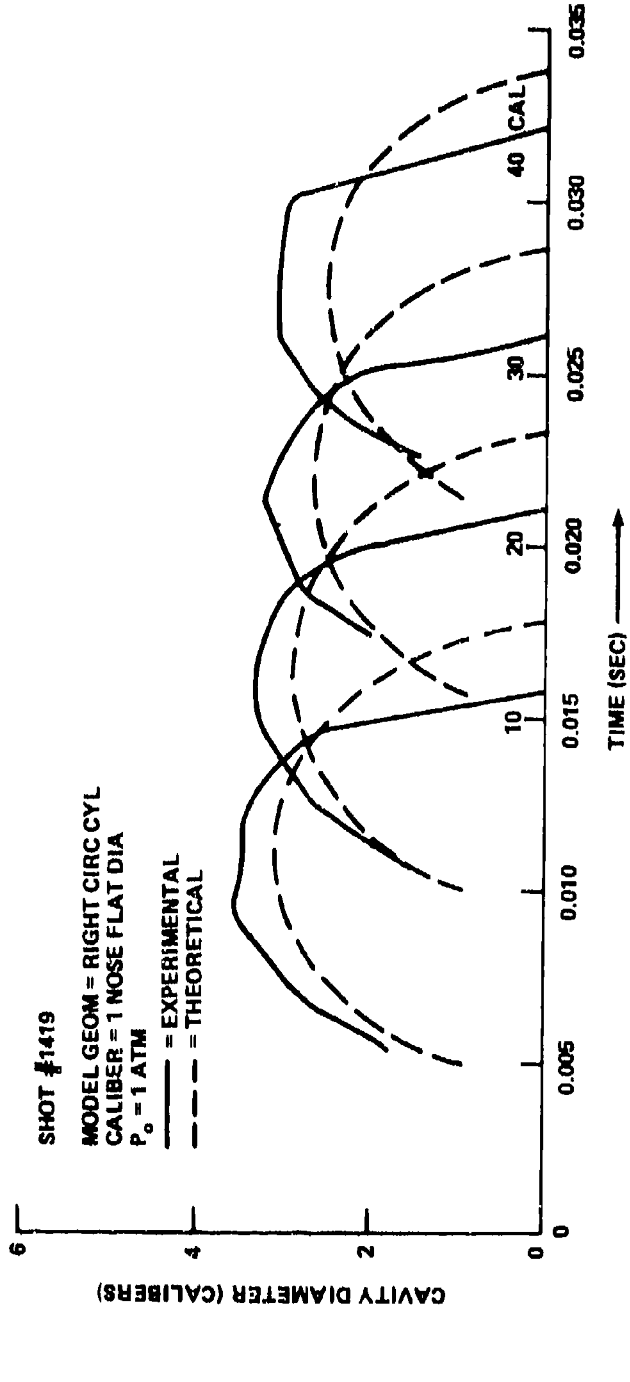

FIGURE 15 CAVITY DIAMETER AT VARIOUS DEPTHS VS TIME

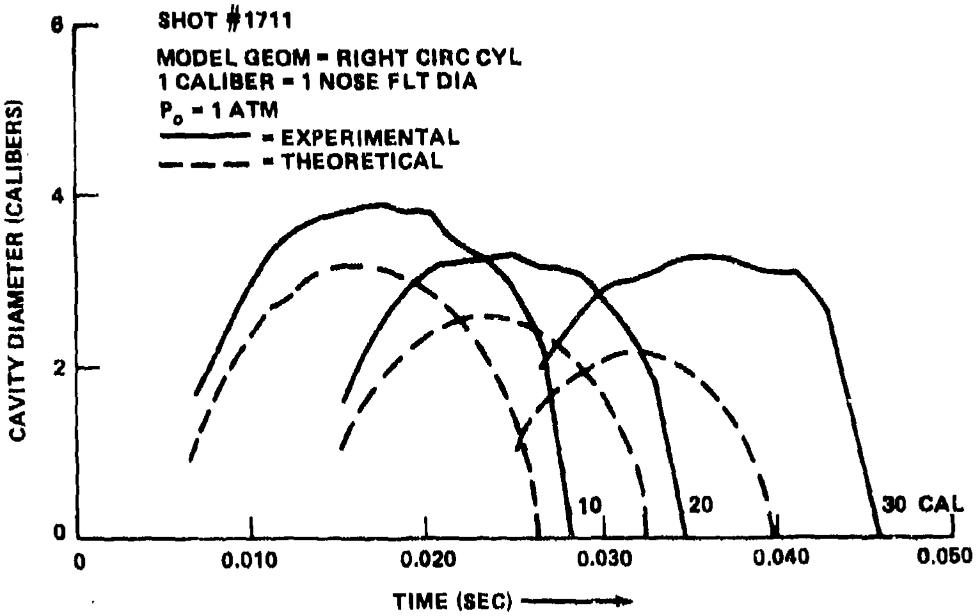

FIGURE 16 CAVITY DIAMETER AT VARIOUS DEPTHS VS TIME

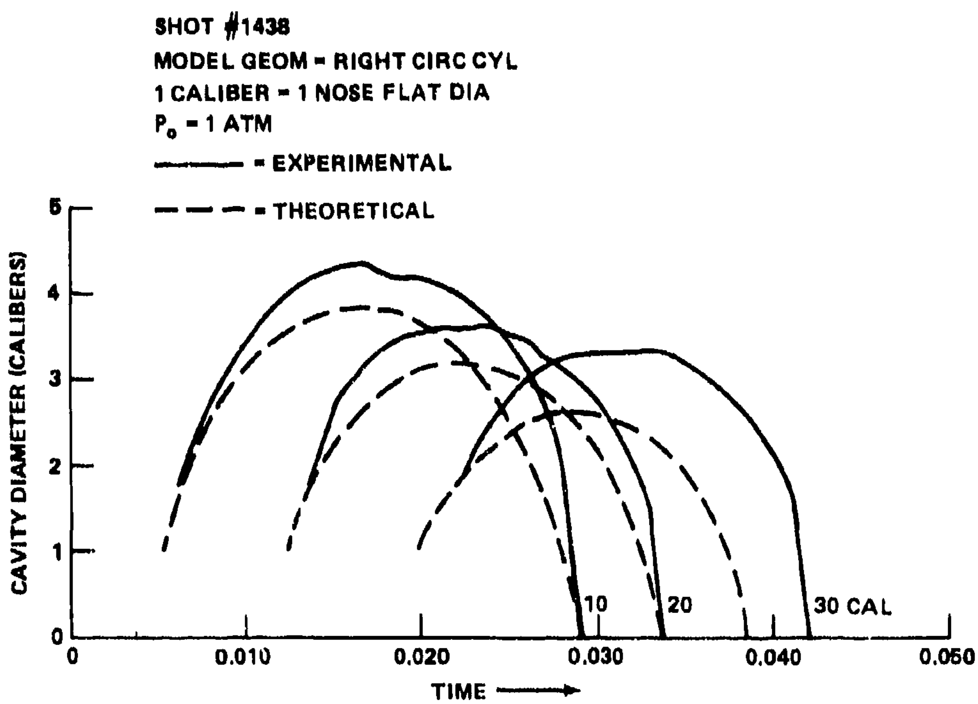

FIGURE 17 CAVITY DIAMETER AT VARIOUS DEPTHS VS TIME

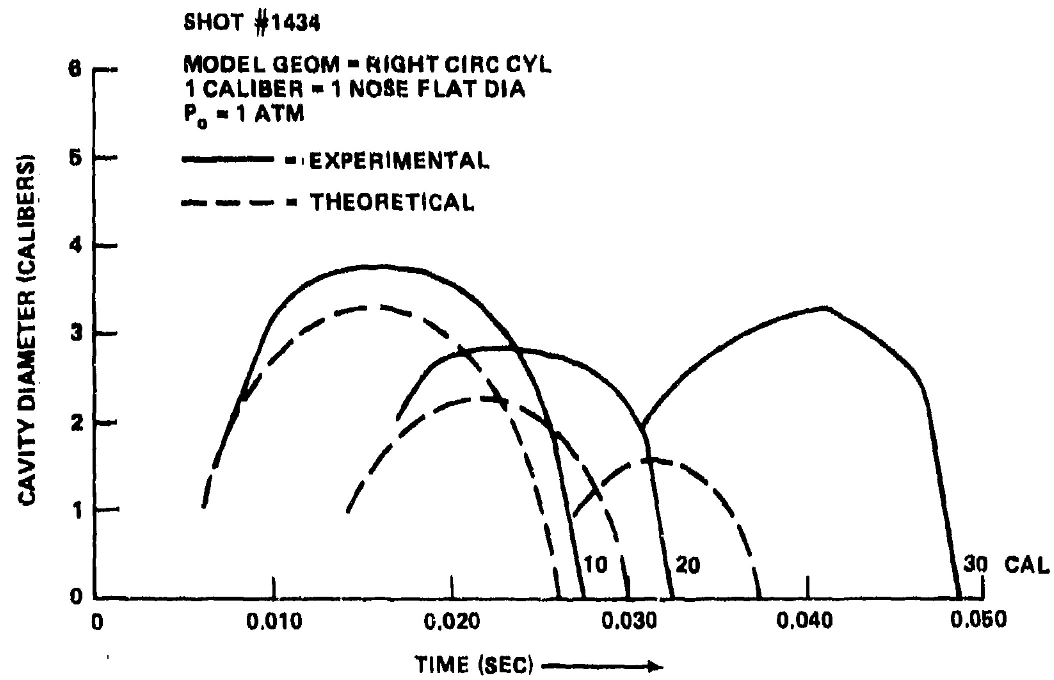

FIGURE 18 CAVITY DIAMETER AT VARIOUS DEPTHS VS TIME

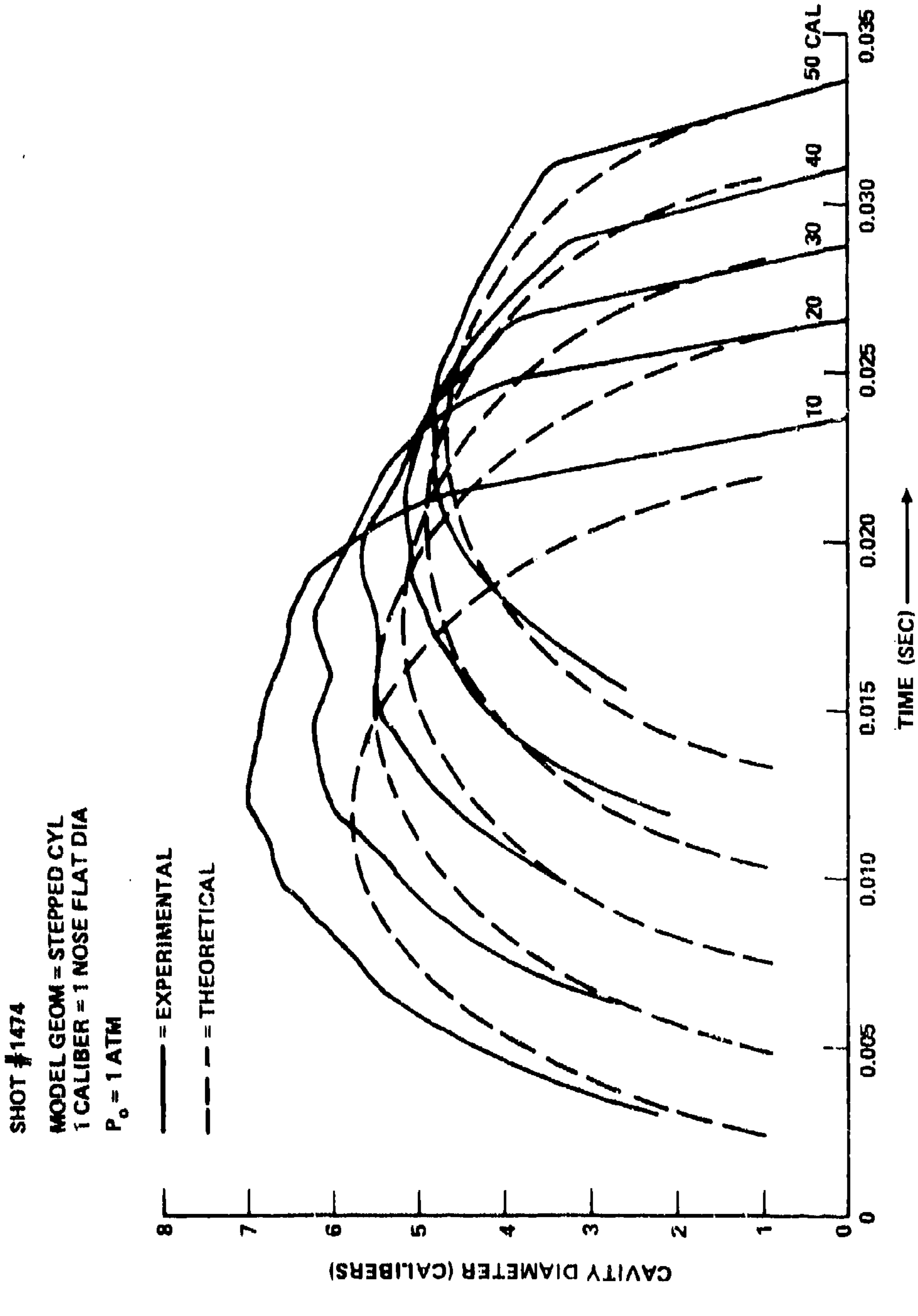

FIGURE 19 CAVITY DIAMETER AT VARIOUS DEPTHS VS TIME

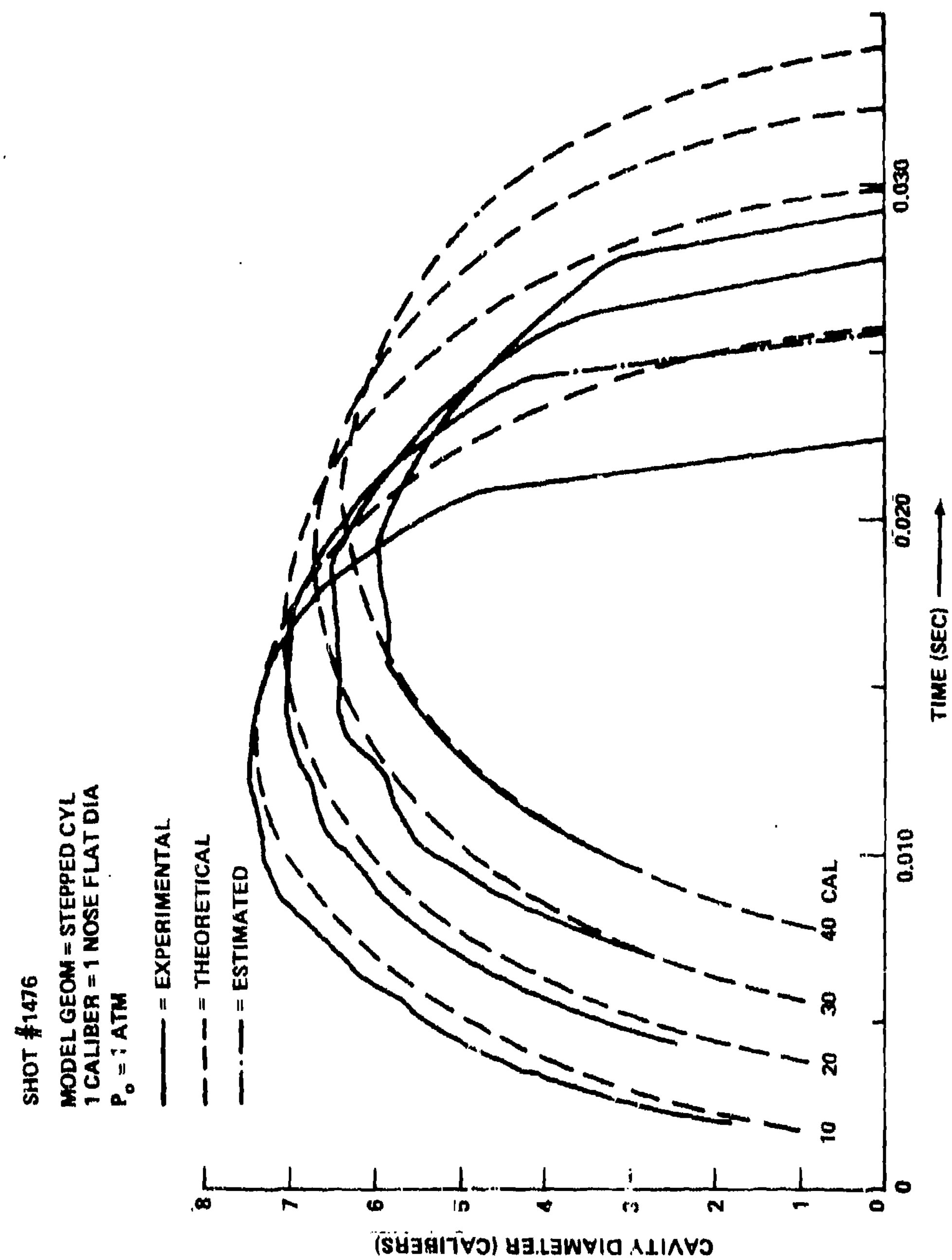

FIGURE 20 CAVITY DIAMETER AT VARIOUS DEPTHS VS TIME

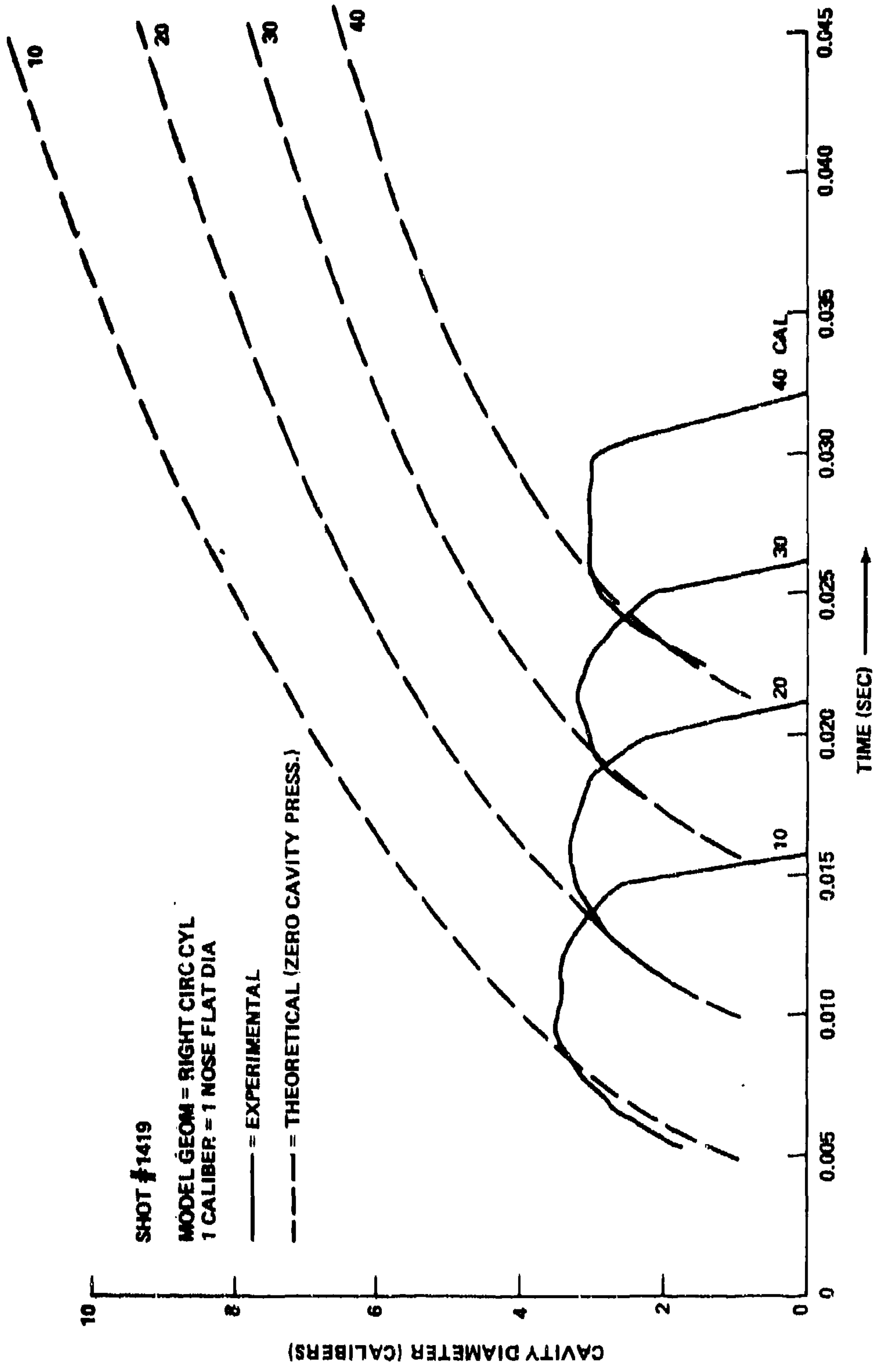

FIGURE 21 CAVITY DIAMETER AT VARIOUS DEPTHS VS TIME

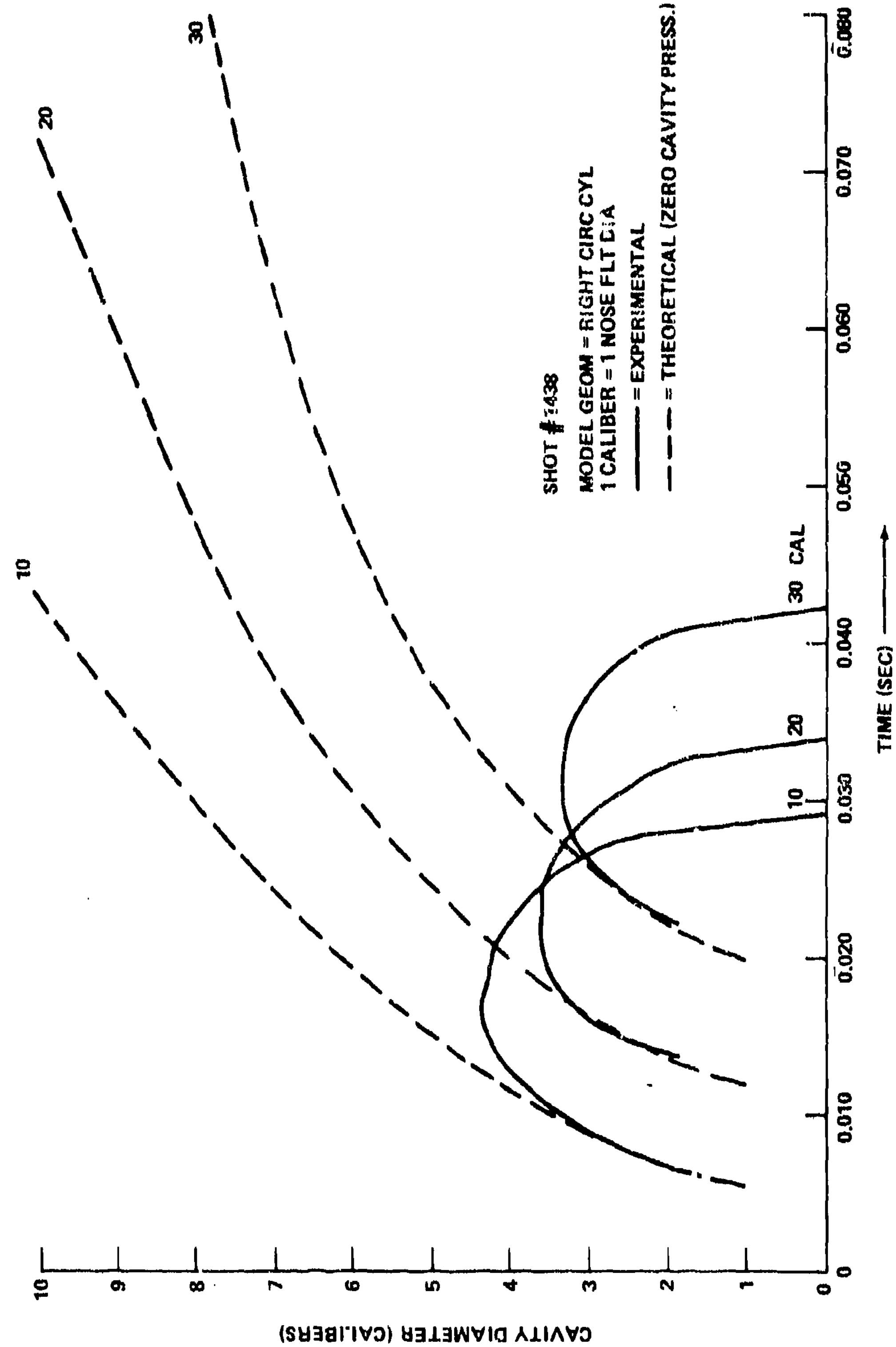

FIGURE 22 CAVITY DIAMETER AT VARIOUS DEPTHS VS TIME

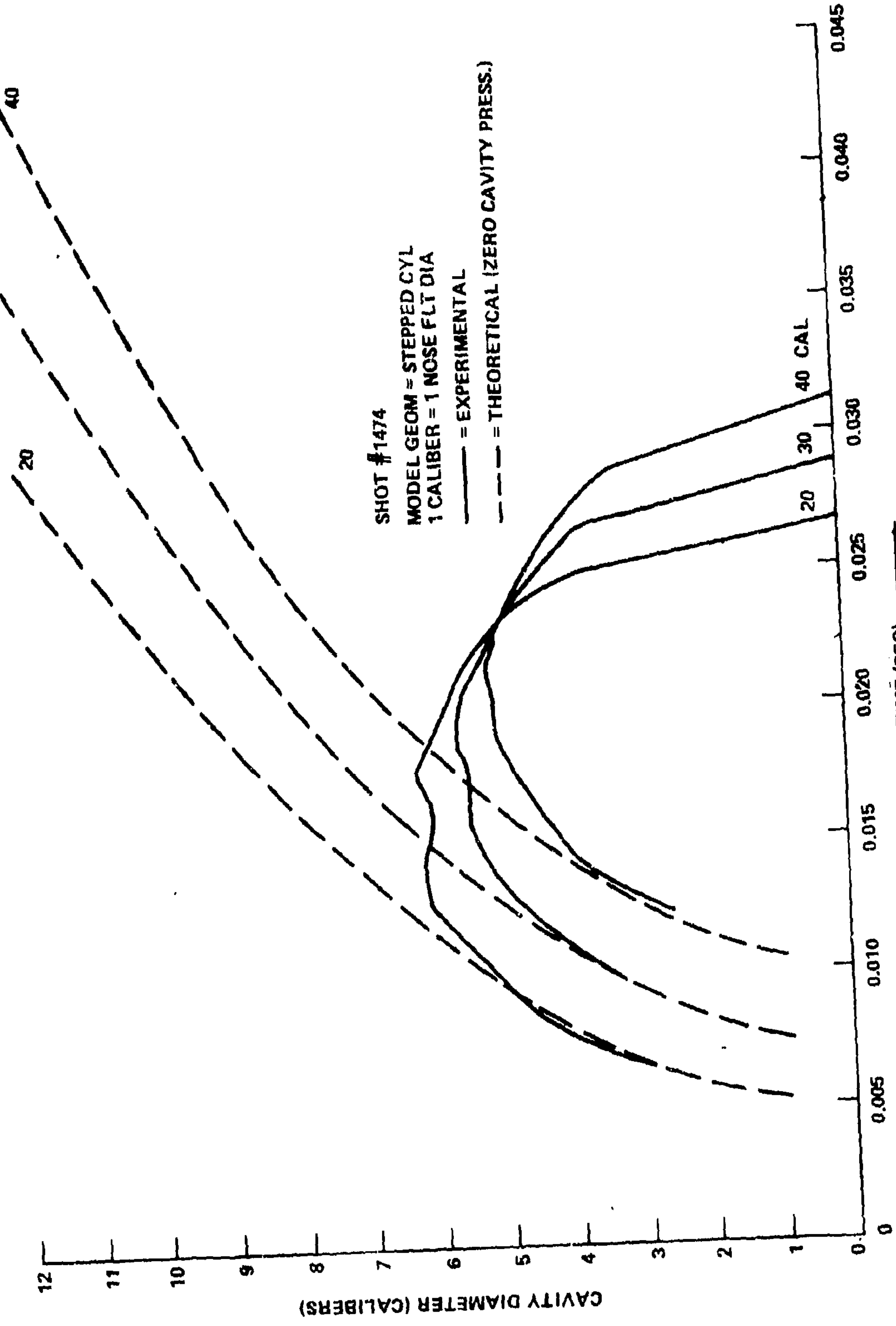

FIGURE 23 CAVITY DIAMETER AT VARIOUS DEPTHS VS TIME

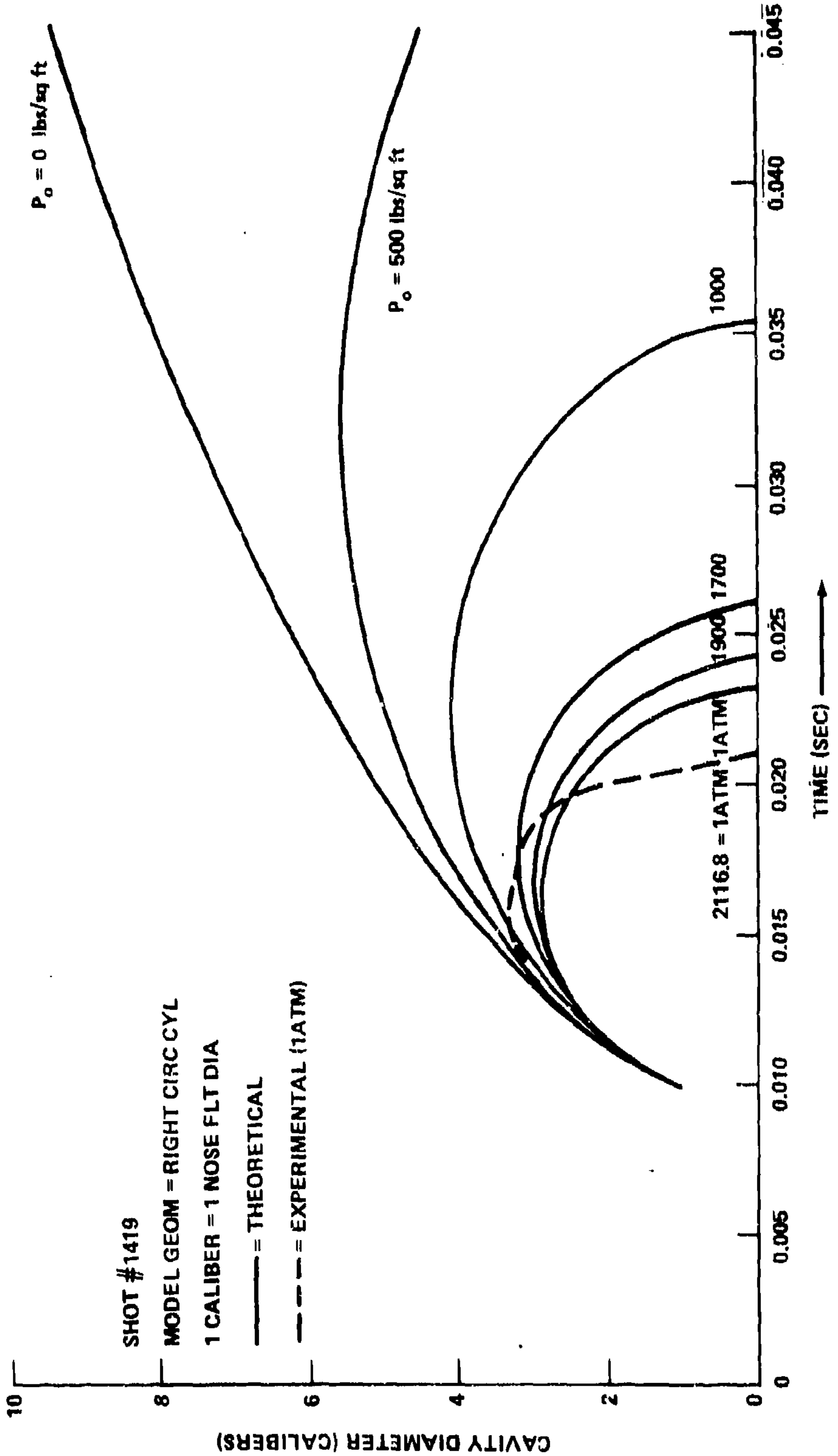

FIGURE 24 CAVITY DIAMETER AT 20 CAL DEPTH VS TIME, FOR VARIOUS SURFACE PRESSURES

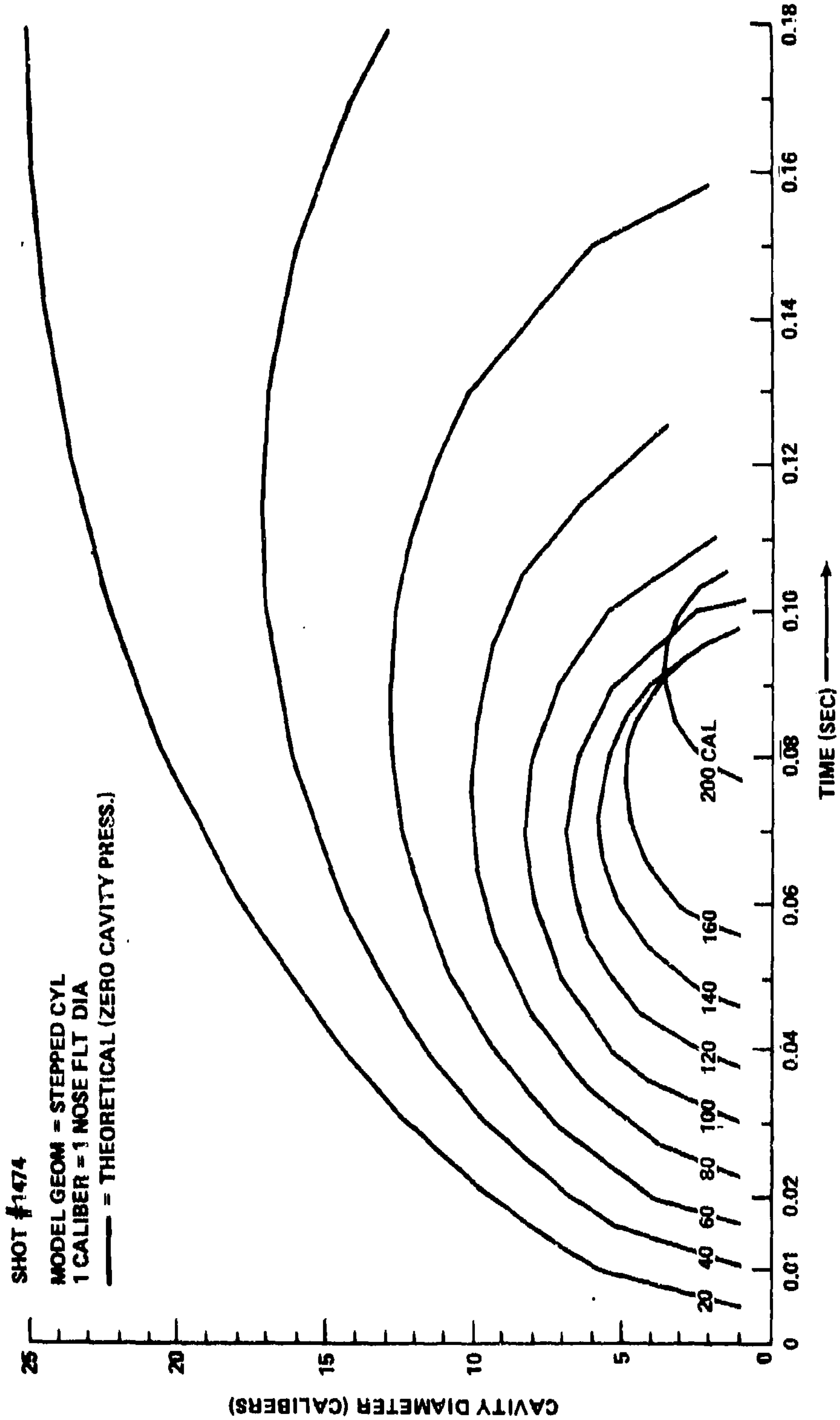

FIGURE 25 CAVITY DIAMETER AT VARIOUS DEPTHS VS. TIME

BIBLIOGRAPHY

Abelson, H., "Cavity Shapes at Vertical Water Entry - A Comparison of Calculated and Observed Shapes," NOLTR 67-31, 1967.

Abelson, H., "The Behavior of the Cavity Formed by a Projectile Entering the Water Vertically," Ph.D. Thesis, Mechanical Engineering, Univ. of MD, 1969.

Birkhoff, G. and Isaac, R., "Transient Cavities in Air-Water Entry," NAVORD 1490, 1951.

May, A., "The Cavity After Vertical Water Entry," NOLTR 68-114, 1968.

May, A. and Hoover, W. R., "A Study of the Water-Entry Cavity," NOLTR 63-264, 1963.

TERMS

A_c	Missile cross-sectional drag area
A_s	Lamina rim surface area
C_D	Cavity drag coefficient of projectile based on A_c
D	Diameter of lamina opening; diameter of cavity at a given depth; missile nose-flat diameter
g	Gravitational acceleration
m_p	Projectile mass
P_o	Atmospheric surface pressure
r	Radius (and "depth") of spherical lamina
r_{cr_1}	First critical minimum depth
r_{cr_2}	Second critical minimum depth
r_p	Projectile depth
R_p	Diameter of axis-symmetric projectile body at zone of separation
t	Elapsed time for missile to reach depth r, measured from entry
T_f	Kinetic energy of fluid in shell
T_p	Kinetic energy of projectile
v_p	Projectile velocity
v_{p_o}	Projectile velocity at water impact
V	Total potential energy of lamina/surface-pressure system
V_g	Potential energy of lamina due to gravity

TERMS (Cont'd)

V_{in}	Initial potential energy of lamina/surface-pressure system in the at-rest (i.e., $\theta_a = 0$) position
V_{peak}	Potential energy of lamina/surface-pressure system when lamina is at peak of its swing (i.e., $\theta_a = \theta_m$)
V_{P_o}	Potential resulting from atmospheric surface pressure
W_{P_o}	Work done by pressure P_o acting on lamina
X, Z	Space saving substitution parameters
α	Retardation coefficient, $\alpha = C_D A_c \rho_w / 2m_p$
θ_a, θ_b	Fluid shell displacement angles
θ_{a_o}	Initial shell angle
θ_m	Maximum possible value of the shell angle θ_a
ρ_w	Density of water

APPENDIX A

PROGRAM LISTING AND SAMPLE OUTPUT

73/74 OPT=1 FTN 4.6+452

```
C                  - P R O G R A M   D E S C R I P T I O N -
C
C
C          THE PROGRAM LISTED BELOW IS DESIGNED TO CARRY OUT A
C     NUMERICAL SOLUTION OF THE THEORETICAL EQUATIONS OF MOTION
C     WHICH APPROXIMATELY PREDICT BEHAVIOR OF WATER ENTRY CAV-
C     ITIES FOR VERTICAL WATER ENTRY.
C          THE EQUATIONS ARE TAKEN FROM A HYDRAULIC CAVITY
C     FLOW MODEL,PROPOSED BY G. BIRKHOFF AND R. ISAACS("TRAN-
C     SIENT CAVITIES IN AIR WATER ENTRY," NAVORD 1490 , 1951),
C     WHICH IS BASED ON THE APPROXIMATE HYPOTHESIS THAT STREAM-
C     LINES LIE ON CONCENTRIC SPHERICAL SURFACES (OR "LAMINAS")
C     CENTERED AT THE POINT OF IMPACT.ANY NOSE CONFIGURATION FOR
C     WHICH THE DRAG COEFF. IS KNOWN MAY BE MODELLED.THE EQUA-
C     TIONS AS USED IN THE PROGRAM HAVE BEEN MODIFIED TO INCLUDE
C     AN ATMOSPHERIC PRESSURE TERM.
C          SPECIFICALLY THE PROGRAM GENERATES "LAMINA PERFOR-
C     MANCE DATA TABLES" FOR THE LAMINAS AT USER SPECIFIED DEPTHS
C     (MEASURED ALONG THE LINE-OF-FIRE),BY MEANS OF A STEP-BY-
C     STEP INTEGRATION OF THE LAMINA MOTION EQNS.COMBINING THE
C     DATA IN THE TABLES FOR LAMINAS AT SEVERAL DEPTHS MAKES IT
C     POSSIBLE TO OBTAIN THE PERFORMANCE HISTORY OF THE OVERALL
C     CAVITY.THE OUTPUT DATA ARE DISPLAYED IN TERMS OF POLAR
C     COORDINATE HOWEVER FOR CONVENIENCE AN APPROXIMATE CAVITY
C     DIAMETER IS COMPUTED AND DISPLAYED BUT IS ACCURATE ONLY
C     FOR SUFFICIENTLY SMALL VALUES OF THE VARIABLE "ANGLE".
C          DIRECTIONS TO SET UP THE INPUT DECK APPEAR BELOW
C     ALONG WITH A DESCRIPTION OF IMPORTANT VARIABLES.THE PRO-
C     GRAM FEATURES A PRINT FREQUENCY PARAMETER,"NSTORE",WHICH
C     AIDS IN REDUCING THE QUANTITY OF OUTPUT PRODUCED.ALSO
C     THE USER NEED NOT BOTHER WITH "MAX ITERATION" OR "MAX TIME"
C     PARAMETERS SINCE,WHEN THE MOTION OF A PARTICULAR LAMINA
C     IS COMPLETED.COMPUTATIONS FOR THAT LAMINA ARE TERMINATED
C     AUTOMATICALLY.
C          PROGRAM AUTHOR- M. A. METZGER , SEPT. 1980
C
C
C
C                           * INPUT DATA *
C
C
C        FIRST CARD -
C
C            VARIABLES = REFDIA,RLNGTH,WEIGHT,RMDRHO,DGAREA,DGCOEF
C          DESCRIPTION = REFERENCE DIAM.(IN.),MODEL LENGTH(IN.),
C                        MODEL WEIGHT(LBS.),MOD. DENS.(LB/CU.IN.),
C                        DRAG AREA(SQ.IN.),DRAG COEFF.,RESP.
C               FORMAT = 6F10.5
C
C
C
C        SECOND CARD -
C
C            VARIABLES = ENTVEL,NDEPTH
C          DESCRIPTION = ENTRY VELOCITY(FPS), NUMBER OF SPECI-
C                        FIED DEPTHS PARAMETER, RESPECTIVELY.
C               FORMAT = F10.5,I5
```

```
C
C
C
C          THIRD SET -
C
C              VARIABLES = DEPTH,DELTA,NSTORE
C            DESCRIPTION = EACH CARD IN THIS SET CONTAINS A USER
C                          SPECIFIED DEPTH ALONG WITH  VALUES FOR
C                          THE DESIRED TIME INCREMENT AND PRINT
C                          FREQUENCY FOR THAT DEPTH.DEPTHS SHOULD
C                          BE IN UNITS OF CALIBERS BASED ON REFDIA.
C                          SUBMIT ONE OF THESE CARDS PER SPECIFIED
C                          DEPTH.
C                 FORMAT = 2F10.5,I5
C
C
C
C
C                                   * VARIABLES *
C
C
C              VARIABLES = ANGLE,ANGVEL,ANGACC
C            DESCRIPTION = ANGLE REPRESENTS THE ANGLE SUBTENDED AT
C                          THE POINT OF ENTRY BY THE LINE-OF-FIRE
C                          AND THE CAVITY WALL AT DEPTH, ANGVEL
C                          AND ANGACC ARE ANGULAR VELOCITY AND
C                          ACCELERATION ASSOCIATTED WITH ANGLE.
C                  TYPES = REAL
C
C
C
C              VARIABLES = WATRHO,PRESSR
C            DESCRIPTION = WATER DENSITY AND ATMOSPHERIC PRESSURE
C                          TERM  RESP.
C                  TYPES = REAL
C
C
C
C
```

```
      PROGRAM CAVITY (INPUT,OUTPUT,TAPE5=INPUT,TAPE6=OUTPUT)
C
C
C     **************************************************
C           PRELIMINARY  OPERATIONS
C     **************************************************
C
      REAL MDMASS , MDLDEP
      DIMENSION DEPTH(10),DELTA(10),NSTORE(10)
      GRAVTY=32.174
      WATRHO=1.93945
      PRESSR=2116.8
      READ(5,1000) REFDIA,RLNGTH,WEIGHT,RMDRHO,DGAREA,DGCOEF
      READ(5,1010) ENTVEL,NDEPTH
      DO 1 I=1,NDEPTH
      READ(5,1020) DEPTH(I),DELTA(I),NSTORE(I)
    1 CONTINUE
C
C
C           * PRINT REFERENCE INFO TABLE *
C
      WRITE(6,2000) REFDIA,RLNGTH,DGCOEF,DGAREA,WEIGHT,
     *               RMDRHO,WATRHO,PRESSR,GRAVTY,ENTVEL,NDEPTH
      REFDIA=REFDIA/12.0
      DGAREA=DGAREA/144.0
      MDMASS=WEIGHT/32.174
      RETARD=(DGCOEF*DGAREA*WATRHO)/(2.0*MDMASS)
      WRITE(6,2005) RETARD
      WRITE(6,2010) (DEPTH(I),I=1,NDEPTH)
      DCONV=180.0/3.141592
C
C
C           * PRINT TABLE HEADING *
C
      WRITE(6,2020)
C
C
C     **************************************************
C           GENERATION  OF   LAMINA
C           PERFORMANCE DATA TABLES
C     **************************************************
C
      DO 50 I=1,NDEPTH
C
C
C           * INITIALIZE PARAMETERS *
C
         ATEMP=RETARD*MDMASS*ENTVEL*ENTVEL*EXP(-2.0*RETARD*DEPTH(I)*
     *         REFDIA)
         BTEMP=2.0*3.141592*(DEPTH(I)**2)*(REFDIA**2)
         CTEMP=DEPTH(I)*REFDIA*WATRHO*GRAVTY+PRESSR
         COSMAX=1.0-ATEMP/(BTEMP*CTEMP)
         DEGANG=ACOS(COSMAX)*180.0/3.141592
         AHTIME=(EXP(RETARD*DEPTH(I)*REFDIA)-1.0)/(RETARD*ENTVEL)
         WRITE(6,2030) DEPTH(I),DELTA(I),NSTORE(I),DEGANG
C
C
```

```
C           * COMPUTE INITIAL ANGLE *
C
            ANGLE=ATAN(1.0/(2.0*DEPTH(I)))
            COSANG=COS(ANGLE)
            SINANG=SIN(ANGLE)
C
C
C           * COMPUTE INITIAL ANG. VEL. *
C
            CALL VELOC(PRESSR,WATRHO,GRAVTY,COSMAX,ANGLE,
     .                 DEPTH(I),REFDIA,ANGVEL)
C
C
C           * COMPUTE INITIAL ANG. ACC. *
C
            CALL ACCEL(PRESSR,WATRHO,GRAVTY,COSMAX,ANGLE,
     .                 DEPTH(I),REFDIA,ANGACC)
C
   20       MOLDEP=ALOG(RETARD*ENTVEL*ABTIME+1.0)/(RETARD*REFDIA)
            CAVDIA=2.0*DEPTH(I)*SIN(ANGLE)
C
C
C           * RADIAN TO DEGREE CONVERSION *
C
            DEGANG=ANGLE*DCONV
            DEGVEL=ANGVEL*DCONV
            DEGACC=ANGACC*DCONV
C
C
C           * PRINT NEXT LINE OF TABLE *
C
            WRITE(6,2040) ABTIME,CAVDIA,DEGANG,
     .                    DEGVEL,DEGACC,MOLDEP
C
C           **********************************************
C                 STEP BY STEP INTEGRATION OF
C                 MOTION EQNS  FOR  LAMINA AT
C                 CURRENT DEPTH(I)
C           **********************************************
C
            OLDANG=ANGLE
            ISTORE=0
   30       ISTORE=ISTORE+1
C
C
C           * COMPUTE NEW ANGLE AND ANGVEL *
C
            ANGLE=OLDANG+ANGVEL*DELTA(I)+0.5*ANGACC*(DELTA(I)**2)
C
C           * CHECK FOR NEG. ANGLE,IF SO *
C             PROCEED TO NEXT DEPTH
C
            IF(ANGLE) 50,40,40
   40       CONTINUE
            CALL VELOC(PRESSR,WATRHO,GRAVTY,COSMAX,ANGLE,
     .                 DEPTH(I),REFDIA,ANGVEL)
            IF(ANGLE.LE.OLDANG) ANGVEL=-ANGVEL
```

```
          OLDANG=ANGLE
C
C
C           * COMPUTE NEW ANG. ACC. *
C
          CALL ACCEL(PRESSR,WATRHO,GRAVTY,COSMAX,ANGLE,
     .               DEPTH(I),REFDIA,ANGACC)
          ABTIME=ABTIME+DELTA(I)
          IF(ISTORE-NSTORE(I)) 30,20,20
   50 CONTINUE
      STOP
C
C
C     ***********************************************
C          FORMAT STATEMENTS
C     ***********************************************
C
 1000 FORMAT(6F10.5)
 1010 FORMAT(F10.5,I5)
 1020 FORMAT(2F10.5,I5)
 2000 FORMAT(1H1,///////,45X,
     .       44H* R E F E R E N C E   I N F O R M A T I O N *,
     .       //////,47X,33HMODEL CONFIGURATION =  SUBROC     ,///,
     .       44X,26HMODEL REF. DIAM. (IN.) =  ,F4.2,//,48X,
     .       22HMODEL LENGTH (IN.) =  ,F5.2,//,50X,
     .       20HCAV. DRAG COEFF. =  ,F5.3,//,43X,
     .       27HEFF. DRAG AREA (SQ.IN.) =  ,F8.5,//,48X,
     .       22HMODEL WEIGHT (LBS) =  ,F8.5,//,40X,
     .       30HMODEL DENSITY (LBS/CU.IN.) =  ,F7.4,//,41X,
     .       29HWATER DENS. (SLUG/CU.FT.) =  ,F7.5,//,42X,
     .       28HATM. PRESS. (LBS/SQ.FT.) =  ,F7.2,//,41X,
     .       29HGRAV. CONST. (FT/SEC/SEC) =  ,F6.3,//,47X,
     .       23HENTRY VEL. (FT/SEC) =  ,F5.1,//,56X,
     .       14HNO. DEPTHS =  ,I2,/)
 2005 FORMAT(1H ,51X,18HRETARD (1/FT.) =  ,F6.5,/)
 2010 FORMAT(1H ,48X,21HDEPTHS (CALIBERS) =  ,F4.1,4F6.1,/)
 2020 FORMAT(1H1,///////,35X,
     .66H- S P H E R I C A L   L A M I N A   P E R F O R M A N C E   D A T
     .A -,///,53X,29HZERO TIME REF. = WATER IMPACT)
 2030 FORMAT(1H ,/////////,34X,27H* * * * * * * * * * * ***   ,
     .       F4.1,38H CAL LAMINA  *** * * * * * * * * * * *,///,
     .       51X,19HTIME STEP (SEC) =  ,F6.5,/,60X,10HNSTORE =  ,
     .       I3,/,51X,19HMAX ANGLE (DEG) =  ,F5.2,///,37X,4HABS.,
     .       8X,7HAPPROX.,15X,4HANG.,8X,4HANG.,8X,5HMODEL,/,37X,
     .       4HTIME,8X,8HCAV.DIA.,2X,5HANGLE,7X,4HVEL.,8X,4HACC.,
     .       8X,5HDEPTH,/,36X,5H(SEC),8X,7H(CAL"S),3X,5H(DEG),
     .       4X,9H(DEG/SEC),3X,10H(DEG/SEC2),4X,7H(CAL"S),/)
 2040 FORMAT(1H ,36X,F5.4, 8X,F5.2,4X,F5.2,4X,F8.2,1X,F14.1,3X,F7.2)
      END
```

SUBROUTINE ACCEL 73/74 OPT=1 FTN 4.6+452 80/1(

```
      SUBROUTINE ACCEL(PRESSR,WATRHO,GRAVTY,COSMAX,ANGLE,
     .                DEPTH,REFDIA,ANGACC)
      COSANG=COS(ANGLE)
      SINANG=SIN(ANGLE)
      X=(2.0-COSANG)*(1.0+COSANG)/(COSANG*(1.0-COSANG))
      RLOGX=ALOG(X)
      A=2.0-4.0*COSANG
      B=RLOGX*COSANG*(2.0+COSANG**3-2.0*COSANG*COSANG-COSANG)
      C=2.0*COSANG/(SINANG*SINANG)
      Z=(A/B)+C
      DUMMY=(1.0+(COSANG-COSMAX)*Z)/(SINANG*RLOGX)
      ANGACC=-2.0*(DEPTH*REFDIA*GRAVTY+PRESSR/WATRHO)*DUMMY/
     .      ((DEPTH*REFDIA)**2)
      RETURN
      END
```

SUBROUTINE VELOC 73/74 OPT=1 FTN 4.6+452 80/1(

```
      SUBROUTINE VELOC(PRESSR,WATRHO,GRAVTY,COSMAX,ANGLE,
     .                DEPTH,REFDIA,ANGVEL)
      COSANG=COS(ANGLE)
      SINANG=SIN(ANGLE)
      X=(2.0-COSANG)*(1.0+COSANG)/(COSANG*(1.0-COSANG))
      RLOG=ALOG(X)
      ANGVEL=SQRT(4.0*(DEPTH*REFDIA*GRAVTY+PRESSR/WATRHO)
     .           *(COSANG-COSMAX)/((DEPTH*REFDIA)**2*SINANG
     .           *SINANG*RLOG))
      RETURN
      END
```

* R E F E R E N C E   I N F O R M A T I O N *

MODEL CONFIGURATION	=	RIGHT CYL.
MODEL REF. DIAM. (IN.)	=	1.50
MODEL LENGTH (IN.)	=	2.15
CAV. DRAG COEFF.	=	.807
EFF. DRAG AREA (SQ.IN.)	=	1.76715
MODEL WEIGHT (LBS)	=	1.07522
MODEL DENSITY (LBS/CU.IN.)	=	.2830
WATER DENS. (SLUG/CU.FT.)	=	1.93945
ATM. PRESS. (LBS/SQ.FT.)	=	2116.80
GRAV. CONST. (FT/SEC/SEC)	=	32.174
ENTRY VEL. (FT/SEC)	=	250.0
NO. DEPTHS	=	3
RETARD (1/FT.)	=	.28737
DEPTHS (CALIBERS)	=	10.0 20.0 30.0

- S P H E R I C A L   L A M I N A   P E R F O R M A N C E   D A T A -

ZERO TIME REF. = WATER IMPACT

* * * * * * * * * * * * *** 10.0 CAL LAMINA *** * * * * * * * * * * * *

TIME STEP (SEC) = .00010
NSTORF = 5
MAX ANGLE (DEG) = 9.45

ABS. TIME (SEC)	APPROX. CAV.DIA. (CAL"S)	ANGLE (DEG)	ANG. VEL. (DEG/SEC)	ANG. ACC. (DEG/SEC2)	MODEL DEPTH (CAL"S)
.0060	1.00	2.86	2524.23	-2148373.6	10.00
.0065	1.37	3.93	1837.22	-911064.9	10.69
.0070	1.66	4.75	1486.39	-548881.7	11.36
.0075	1.89	5.43	1257.18	-386432.5	12.02
.0080	2.10	6.02	1088.26	-297256.2	12.66
.0085	2.27	6.53	954.43	-242139.3	13.29
.0090	2.43	6.97	843.15	-205324.0	13.90
.0095	2.57	7.37	747.34	-179366.2	14.50
.0100	2.69	7.72	662.66	-160333.9	15.09
.0105	2.80	8.03	586.25	-145974.0	15.67
.0110	2.89	8.31	516.15	-134912.2	16.23
.0115	2.97	8.55	450.94	-126269.1	16.78
.0120	3.05	8.76	389.58	-119459.8	17.32
.0125	3.11	8.94	331.25	-114083.9	17.86
.0130	3.16	9.09	275.31	-109861.4	18.38
.0135	3.20	9.22	221.24	-106594.0	18.89
.0140	3.24	9.31	168.59	-104140.8	19.39
.0145	3.26	9.39	116.96	-102403.2	19.89
.0150	3.28	9.43	66.08	-101314.7	20.37
.0155	3.28	9.45	15.57	-100835.6	20.85
.0160	3.28	9.45	-25.66	-100883.8	21.32
.0165	3.28	9.42	-76.22	-101482.8	21.78
.0170	3.26	9.37	-127.24	-102697.1	22.23
.0175	3.23	9.30	-179.02	-104571.7	22.68
.0180	3.20	9.19	-231.93	-107178.7	23.12
.0185	3.15	9.07	-286.34	-110624.3	23.55
.0190	3.10	8.91	-342.71	-115059.4	23.98
.0195	3.03	8.72	-401.59	-120696.5	24.40
.0200	2.96	8.51	-463.65	-127835.9	24.81
.0205	2.87	8.26	-529.74	-136908.7	25.22
.0210	2.77	7.98	-600.98	-148547.8	25.62
.0215	2.66	7.66	-678.86	-163711.7	26.01
.0220	2.54	7.30	-765.51	-183911.0	26.40
.0225	2.40	6.89	-864.00	-211650.8	26.79
.0230	2.24	6.43	-979.11	-251366.2	27.17
.0235	2.06	5.91	-1118.70	-311619.8	27.54
.0240	1.85	5.30	-1297.04	-411041.0	27.91
.0245	1.60	4.60	-1543.69	-597968.7	28.28
.0250	1.30	3.74	-1934.54	-1040086.3	28.64
.0255	.91	2.60	-2769.24	-2802135.3	28.99
.0260	.12	.34	********	-862860962.9	29.34

* * * * * * * * * * * * * *** 20.0 CAL LAMINA *** * * * * * * * * * * * *

TIME STEP (SEC) = .00010
NSTORE = 5
MAX ANGLE (DEG) = 3.24

ABS. TIME (SEC)	APPROX. CAV.DIA. (CAL"S)	ANGLE (DEG)	ANG. VEL. (DEG/SEC)	ANG. ACC. (DEG/SEC2)	MODEL DEPTH (CAL"S)
.0146	1.00	1.43	760.50	-455800.2	20.00
.0151	1.23	1.77	590.90	-257576.3	20.48
.0156	1.42	2.03	484.92	-176413.0	20.96
.0161	1.57	2.26	408.34	-133996.1	21.43
.0166	1.71	2.44	348.19	-108615.4	21.88
.0171	1.82	2.60	298.29	-92084.1	22.34
.0176	1.91	2.74	255.27	-80692.8	22.78
.0181	2.00	2.86	217.08	-72541.1	23.22
.0186	2.07	2.96	182.38	-66566.6	23.65
.0191	2.12	3.04	150.26	-62136.2	24.07
.0196	2.17	3.11	120.06	-58854.9	24.49
.0201	2.21	3.16	91.26	-56469.1	24.90
.0206	2.23	3.20	63.47	-54814.1	25.31
.0211	2.25	3.23	36.35	-53785.4	25.71
.0216	2.26	3.24	9.60	-53321.9	26.10
.0221	2.26	3.24	-14.93	-53371.1	26.49
.0226	2.25	3.22	-41.73	-53944.5	26.88
.0231	2.23	3.20	-68.97	-55092.4	27.25
.0236	2.20	3.15	-96.93	-56883.6	27.63
.0241	2.16	3.10	-125.97	-59433.1	28.00
.0246	2.11	3.03	-156.51	-62920.4	28.36
.0251	2.05	2.94	-189.09	-67622.3	28.72
.0256	1.98	2.84	-224.40	-73971.5	29.07
.0261	1.90	2.72	-263.44	-82667.5	29.42
.0266	1.80	2.57	-307.64	-94896.9	29.77
.0271	1.68	2.41	-359.26	-112815.1	30.11
.0276	1.54	2.21	-422.07	-140719.8	30.45
.0281	1.38	1.98	-503.15	-188392.3	30.78
.0286	1.19	1.71	-617.90	-283058.5	31.11
.0291	.94	1.35	-809.73	-532201.3	31.43
.0296	.60	.85	-1296.35	-1912956.5	31.75

* * * * * * * * * * * * *** 30.0 CAL LAMINA *** * * * * * * * * * * *

TIME STEP (SEC) = .00010
NSTORE = 5
MAX ANGLE (DEG) = 1.48

ABS. TIME (SEC)	APPROX. CAV.DIA. (CAL"S)	ANGLE (DEG)	ANG. VEL. (DEG/SEC)	ANG. ACC. (DEG/SEC2)	MODEL DEPTH (CAL"S)
.0270	1.00	.95	288.82	-140130.4	30.00
.0275	1.13	1.08	230.10	-99634.3	30.34
.0280	1.24	1.19	186.17	-78150.5	30.67
.0285	1.33	1.27	150.56	-65303.5	31.00
.0290	1.40	1.34	120.12	-57071.8	31.33
.0295	1.46	1.39	93.05	-51608.7	31.65
.0300	1.50	1.43	68.22	-47969.1	31.97
.0305	1.53	1.46	44.87	-45637.5	32.29
.0310	1.55	1.48	22.42	-44328.6	32.60
.0315	1.55	1.48	.41	-43897.3	32.91
.0320	1.55	1.48	-21.61	-44297.9	33.21
.0325	1.53	1.46	-44.03	-45572.7	33.51
.0330	1.50	1.43	-67.34	-47863.0	33.81
.0335	1.46	1.39	-92.10	-51447.5	34.11
.0340	1.40	1.34	-119.08	-56830.8	34.40
.0345	1.33	1.27	-149.37	-64936.6	34.69
.0350	1.25	1.19	-184.75	-77564.2	34.97
.0355	1.14	1.09	-228.29	-98613.0	35.26
.0360	1.01	.96	-286.29	-138067.7	35.54
.0365	.83	.80	-374.45	-229697.3	35.82
.0370	.60	.57	-552.06	-575368.9	36.09
.0375	.15	.14	-2170.53	-31522971.7	36.36

BLANK PAGE

APPENDIX B

DERIVATION OF LAMINA MOTION EQUATIONS WHICH INCLUDE EFFECT OF ATMOSPHERIC SURFACE PRESSURE

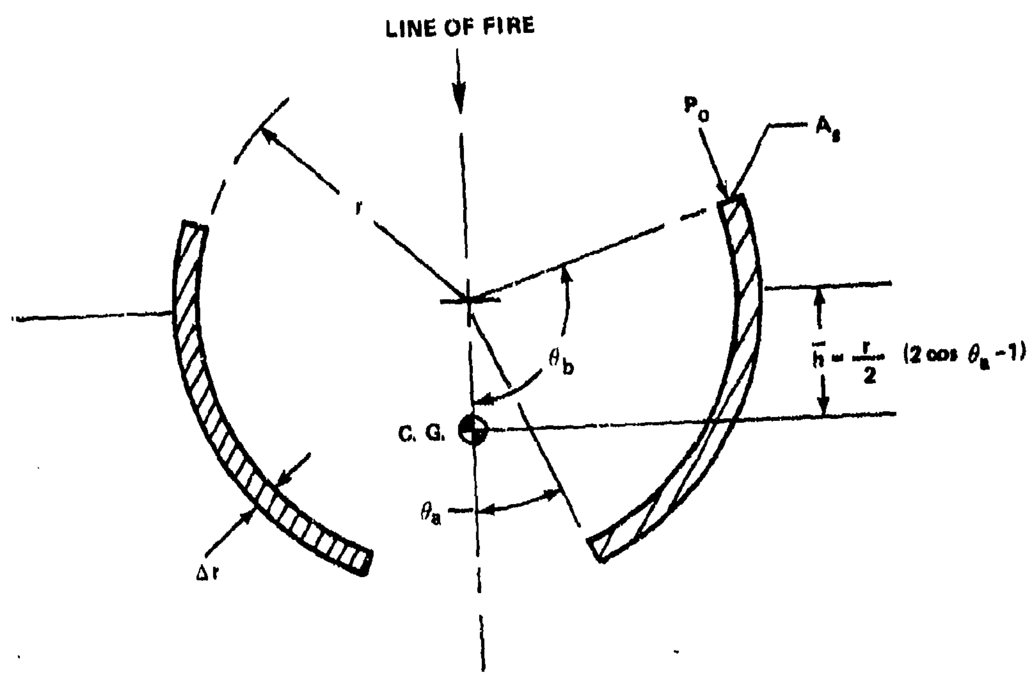

This derivation uses an energy-approach to obtain the equations governing the motion of the lamina. Refer to the figure above throughout the derivation.

First, obtain expression for the potential due to surface pressure P_o, which is equal to negative of the work done by P_o moving thru the displacement $(\theta_b - 90^o)$:

$$dV_{P_o} = - dW_{P_o} = - (- P_o A_s \, r \, d\theta_b) \tag{1}$$

where the area A_s, as shown in the figure, is given by:

$$A_s = 2\pi r \, \Delta r \sin \theta_b$$

Substitute expression for A_s into Equation (1) and integrate to obtain an equation for V_{P_o} in terms of θ_b, thus:

$$\int_{V=0}^{V=V_{P_o}} dV_{P_o} = \int_{\theta_b = 90^o}^{\theta_b} P_o \, 2\pi \, r^2 \, \Delta r \sin \theta_b \, d\theta_b$$

$$V_{P_o} = - 2\pi \, r^2 \, \Delta r \, P_o \cos \theta_b \Big|_{90^o}^{\theta_b}$$

or:

$$V_{P_o} = - 2\pi \, r^2 \, \Delta r \, P_o \cos \theta_b \tag{2}$$

It can be shown that:

$$\cos \theta_b = \cos \theta_a - 1$$

Substituting this into Equation (2) yields the expression for V_{P_o} in terms of angle θ_a:

$$V_p = - 2 \quad r^2 \quad r \, P_o \, (\cos \quad _a - 1) \tag{3}$$

Next consider gravity potential V_g. If the original undisturbed water surface is taken as the reference datum for zero gravity potential then

$$V_g = -2\pi r^2 \Delta r \rho_w g \bar{h}$$

where, as shown in figure:

$$\bar{h} = r(2 \cos \theta_a - 1)/2$$

Hence gravity potential in terms of shell angle is

$$V_g = \pi r^3 \rho_w \Delta r g (1 - 2 \cos \theta_a)$$

Finally, combine potentials due to gravity and surface pressure to obtain the total potential of the shell/pressure system

$$V = V_g + V_{p_o}$$

$$V = \pi r^3 \rho_w \Delta r g (1 - 2 \cos \theta_a) - 2\pi r^2 \Delta r p_o (\cos \theta_a - 1) \tag{4}$$

Next, consider the kinetic energy of the moving shell. In terms of the shell angle θ_a, the expression for the kinetic energy can be shown to be[A-1]

$$T_f = \frac{\pi}{2} r^4 \rho_w \Delta r \dot{\theta}_a^2 \sin^2 \theta_a \ln \left[\frac{(2 - \cos \theta_a)(1 + \cos \theta_a)}{\cos \theta_a (1 - \cos \theta_a)}\right] \tag{5}$$

For the total energy in the conservative shell/surface-pressure system the following relation holds at all times

$$(T_f + V)_1 = (T_f + V)_2 = \text{Const.} \tag{6}$$

When the shell is at the peak of its swing, its kinetic energy is zero and the total potential of the system is at a maximum which, from Equation (6), is equal to the total energy of the shell at any other time.

$$(T_f + V) = V(\text{peak}) \tag{7}$$

At the peak position θ_a is also at a maximum and is designated as θ_m, the maximum value that θ_a ever reaches. When the previously derived expressions for T_f and V are substituted into Equation (7) and the shell angle in the expression for V(peak) is replaced by θ_m, Equation (7) becomes

[A-1]Abelson, H., "Cavity Shapes at Vertical Water Entry - A Comparison of Calculated and Observed Shapes," NOLTR 67-31 (1967).

$$\frac{\pi}{2}\, r^4 \rho_w\, (\Delta r)\, \dot{\theta}_a^2 \sin^2 \theta_a \ln [X] + \pi r^3\, (\Delta r)\, \rho_w\, g\, (1 - 2\cos\theta_a)$$

$$- 2\pi r^2\, (\Delta r)\, P_o\, (\cos\theta_a - 1)$$

$$= \pi r^3 \rho_w\, (\Delta r)\, g\, (1 - 2\cos\theta_m) - 2\pi r^2\, (\Delta r)\, P_o\, (\cos\theta_m - 1)$$

where

$$X = (2 - \cos\theta_a)\,(1 + \cos\theta_a)/\cos\theta_a\,(1 - \cos\theta_a)$$

Solving this last expression for the angular veloctiy $\dot{\theta}_a$ yields the governing differential equation for the shell angle

$$\dot{\theta}_a = \pm \sqrt{\frac{4\left[rg + (P_o/\rho_w)\right]\left[\cos\theta_a - \cos\theta_m\right]}{r^2 \sin^2\theta_a \ln\left[\dfrac{(2-\cos\theta_a)\,(1+\cos\theta_a)}{\cos\theta_a\,(1-\cos\theta_a)}\right]}} \tag{8}$$

The expression for angular acceleration $\ddot{\theta}_a$ can be found by differentiating Equation (8) with respect to time

$$\ddot{\theta}_a = \frac{-2\left[rg + (P_o/\rho_w)\right]}{r^2}\left[\frac{1 + (\cos\theta_a - \cos\theta_m)\,(Z)}{\sin\theta_a \ln [X]}\right]$$

$$X = \frac{(2 - \cos\theta_a)\,(1 + \cos\theta_a)}{\cos\theta_a\,(1 - \cos\theta_a)} \tag{9}$$

$$Z = \frac{2 - 4\cos\theta_a}{\cos\theta_a\,(\cos^3\theta_a - 2\cos^2\theta_a - \cos\theta_a + 2)\ln[X]} + \frac{2\cos\theta_a}{\sin^2\theta_a}$$

The expression for $\cos\theta_m$ is derived next. At the peak of its outward swing (corresponding to $\theta_a = \theta_m$) all the kinetic energy imparted initially to the lamina by the passing projectile has been converted entirely into potential energy thus:

$$V_{peak} - V_{in} = \frac{-dT_p}{dr}\,(\Delta r) \tag{10}$$

where T_p, the kinetic energy of the projectile, is given by

$$T_p = \frac{1}{2}\, m_p\, v_p^2$$

If the cavity drag coefficient is assummed to be constant then T_p can be written in terms of lamina depth r as

$$T_p = \frac{1}{2} m_p v_{p_o}^2 e^{-2\alpha r}$$

The expressions for T_p, V_{peak} and V_{in} are substituted into Equation (10) and the differentiation carried out to obtain

$$\pi r^3 \rho (\Delta r) g (1 - 2 \cos \theta_m) - (-\pi r^3 \rho_w (\Delta r) g)$$

$$- 2\pi r^2 (\Delta r) P_o (\cos \theta_m - 1) = \alpha m_p v_{p_o} e^{-2\alpha r} (\Delta r)$$

Solving for cos θ_m yields the final desired relation

$$\cos \theta_m = \frac{1}{2} \left[2 - \frac{\alpha m_p v_{p_o} e^{-2\alpha r}}{\pi r^2 (r \rho_w g + P_o)} \right] \qquad (11)$$

BLANK PAGE

DISTRIBUTION

	Copies
Commander Naval Sea Systems Command Attn: SEA-09G32	2
SEA-03B	1
SEA-63R31, T. Peirce	1
Department of the Navy Washington, DC 20362	
Office of Naval Research Attn: Code 438	2
800 N. Quincy St. Arlington, VA 22217	
Library of Congress Attn: Gift and Exchange Division	4
Washington, DC 20540	
Defense Technical Information Center Cameron Station Alexandria, VA 22314	12
Director Defense Research and Engineering The Pentagon Washington, DC 20301	1
Director of Research National Aeronautics and Space Administration 600 Independence Avenue, SW Washington, DC 20546	1
NASA Scientific and Technical Information Facility P.O. Box 33 College Park, MD 20740	1
Director Alden Research Laboratories Worchester Polytechnic Institute Holden, MA 01520	1
Applied Physics Laboratory The Johns Hopkins University Attn: Document Librarian	1
Johns Hopkins Road Laurel, MD 20810	
Applied Research Laboratory The Pennsylvania State University Attn: Library	1
Dr. J. W. Holl	1
P.O. Box 30 State College, PA 16801	
Superintendent U.S. Naval Postgraduate School Attn: Library	1
Monterey, CA 93940	
Commanding Officer U.S. Naval Air Development Center Attn: NADC Library	1
Warminister, PA 18974	
Director U.S. Naval Research Laboratory Attn: Library	1
Washington, DC 20390	
Commanding Officer David Taylor Naval Ship Research and Development Center Attn: Library	1
Bethesda, MD 20084	

DISTRIBUTION (Cont.)

	Copies
Commander Naval Ocean Systems Center San Diego, CA 92132	1
Commanding Officer Naval Underwater Systems Center Newport, RI 02840	1
Commander Naval Weapons Center Attn: Library China Lake, CA 93555	1
Harry Diamond Laboratories 2800 Powder Mill Road Adelphi, MD 20783	1
Hydronautics, Inc. Pindell School Road Laurel, MD 20810	1
Iowa Institute of Hydraulic Research State University of Iowa Iowa City, IA 52240	1
California Institute of Technology Pasadena, CA 91109	1
Massachusetts Institute of Technology Cambridge, MA 02139	1

TO AID IN UPDATING THE DISTRIBUTION LIST FOR NAVAL SURFACE WEAPONS CENTER, WHITE OAK TECHNICAL REPORTS PLEASE COMPLETE THE FORM BELOW:

TO ALL HOLDERS OF NSWC TR 81-59
By M. A. Metzger, Code K23

DO NOT RETURN THIS FORM IF ALL INFORMATION IS CURRENT

A. FACILITY NAME AND ADDRESS (OLD) (Show Zip Code)

NEW ADDRESS (Show Zip Code)

B. ATTENTION LINE ADDRESSES:

C.

☐ REMOVE THIS FACILITY FROM THE DISTRIBUTION LIST FOR TECHNICAL REPORTS ON THIS SUBJECT.

D.

NUMBER OF COPIES DESIRED ______________________

DEPARTMENT OF THE NAVY
NAVAL SURFACE WEAPONS CENTER
WHITE OAK, SILVER SPRING, MD. 20910

OFFICIAL BUSINESS
PENALTY FOR PRIVATE USE, $300

POSTAGE AND FEES PAID
DEPARTMENT OF THE NAVY
DOD 316

COMMANDER
NAVAL SURFACE WEAPONS CENTER
WHITE OAK, SILVER SPRING, MARYLAND 20910

ATTENTION: CODE K23